infrastructures

MDPI

Article

Valorization of Multi-Waste Materials in Eco-Friendly Engineered Cementitious Composites

Rabie A. M. Amnisi [1,2], Mohamed E. El-Zoughiby [1], Basem S. Abdelwahed [1] and Osama Youssf [3,1,*]

[1] Structural Engineering Department, Mansoura University, Mansoura 35516, Egypt
[2] Department of Structure Engineering, University of Derna, Alqubah 0810, Libya
[3] Civil and Environmental Engineering Department, United Arab Emirates University, Al Ain 15551, United Arab Emirates
* Correspondence: osama.youssf@mymail.unisa.edu.au

Abstract

Engineered cementitious composite (ECC) is an advanced material known for its superior flexibility, high durability, and crack resistance, making it ideal for a variety of structural applications. However, it uses cement at a rate of 2–3 times more than conventional concrete which raises environmental concerns. This study focused on the production of eco-friendly ECC by incorporating various waste materials as partial cement and sand substitutes. Cement kiln dust (CKD), ceramic powder waste (CPW), and eggshell waste (ESW) were used as partial substitutes for cement in doses of 10% and 20%. Crumb rubber (CR) was used as a partial substitute for sand in doses of 25, 50, 75, and 100%. Chemical treatments using sodium hydroxide, sodium silicate, and a mix of both of them were carried out for the CR in the production of the proposed ECC. Physical treatment using the same cement substitute materials (CKD, CP and ESP) was also carried out for the CR. The effect of fiber type—such as basalt fibers (BF), polypropylene fibers (PPF), and steel fibers (S_tF)—on the performance of ECC was also investigated. Slump, compressive strength, uniaxial tensile strength, flexural strength, and sorptivity were the measured properties for the proposed ECC. Microstructure analyses were also conducted on some selected ECC mixtures. Among the tested mixtures, the results showed that replacing 10% of the cement with CKD improved the compressive strength by up to 22.6% and the tensile strength by up to 18.3%. Using 50% untreated CR reduced compressive and tensile strength by 32.8% and 28.1%, respectively, compared to the control ECC. The physical treatment of CR using CKD improved the compressive strength by up to 12.7% and the tensile strength by up to 3.2% compared to untreated CR. The microstructure analyses revealed an improvement in fiber-matrix bonding and a reduction in crack width in the mixtures, especially in the BF and PPF blends.

Keywords: ECC; cement kiln dust; ceramic powder waste; eggshell waste; crumb rubber

Check for updates

Academic Editor: Ali Behnood

Received: 23 February 2026
Revised: 18 March 2026
Accepted: 21 April 2026
Published: 28 April 2026

Copyright: © 2026 by the authors. Licensee MDPI, Basel, Switzerland. This article is an open access article distributed under the terms and conditions of the Creative Commons Attribution (CC BY) license.

1. Introduction

The engineered cement composite (ECC) is one of the types of high-performance building materials, discovered in the early 1990s by Li [1]. To improve effective cooperation between the fibers, matrix, and ECC components, efforts were made to develop them based on the principles of micromechanics theory. The tensile strain capacity of ECC ranges from 2% to 10%, which is significantly higher than the 0.01% often found in conventional concrete [2–5]. One of the advantages of ECC is the formation of numerous fine cracks,

accompanied by its ability to harden under tension, which significantly contributes to the durability of ECC structures to a level that far exceeds that observed in traditional concrete structures [6–10]. Therefore, the combination of rapid population growth and limited buildable land has led to extremely dense urban environments, and resorting to tall structures significantly enhances the energy absorption properties of concrete [11,12]. Based on this, numerous investigations have been carried out to improve the ductility, toughness, and resilience of structures by replacing ECC with traditional concrete and verifying them [13–20].

Over the past ten years, in several construction applications, the performance of crumb rubber concrete (CRC) has become a hot topic in structural and civil engineering [21]. One of the current environmental problems facing the world today is the disposal of used tires. Nearly a billion tires reach the end of their usable life each year, and at least half of them are discarded untreated. By 2030, that number is predicted to increase to 1.2 billion tires every year. In addition to the stored quantities, we would need to regularly dispose of approximately five billion tires. Incineration has proven to provide significant environmental pollution and fire hazards. Similarly, the consumption of readily available areas and the health hazards caused by rodents and other insects have made landfill disposal difficult [22–24]. Concrete that incorporates rubber in its manufacturing has properties that distinguish it from traditional concrete. Higher damping qualities, greater ductility, superior resistance to impact and toughness, lightweight, and high acoustic and thermal insulation capabilities are some examples of these characteristics [25]. Because of its low compressive strength, rubberized concrete has primarily been used for non-structural components that are prone to impact or vibrations, such as railroad tracks, pipe caps, and traffic barriers.

The replacement of crumb rubber (CR) as fine aggregate in conventional concrete and mortar mixes has been the subject of numerous investigations. Nevertheless, these investigations substituted some of the silica sand in advanced cementitious concrete with ground rubber in engineered cementitious concrete (ECC). Therefore, none of the previous studies used recycled rubber as a complete (100%) substitute for traditional sand as aggregate. The impact of untreated crumb rubber on up to 100% of the characteristics of ECC was examined by Adeyemi Adesina et al. [26]. Similarly, Huang et al. [27] introduced shredded rubber as a substitute for iron ores (i.e., not silica sand) in ECC mixtures, and no study was conducted on the bending and permeability properties of the resulting compounds. These investigations, with their limited scope, were unable to understand the overall performance of the ECC mix that incorporates recycled treatment rubber, especially those that incorporate recycled rubber at up to 100% as a substitute for sand. Therefore, this research was carried out to present a comprehensive study to identify the impact of using CR as a sand substitute at a rate of up to 100% on the performance of ECC mixtures. Both mechanical properties and sulphate resistance were evaluated for 180 days in the present research, with exposure periods extended to over 365 days and complemented with data on ultrasonic pulse velocity (UPV), mass change rate, and wear resistance in the subsequent study.

Numerous investigations have been carried out to treat the rubber surface with sodium hydroxide (NaOH) [28,29], cement paste as a coating layer [30], ultraviolet radiation [31], and simple water washes in order to address the strength loss caused by the rubber surface's poor adherence [32]. Through treatment with heating of the rubber, the loss of compressive strength was retrieved by 93%, 60%, and 47% when using rubber at 10%, 20%, and 30%, respectively [33]. Another study presented five different methods for treating rubber surfaces: sodium hydroxide, sulfuric acid soaking, silica dust, cement coating, and potassium permanganate [34]. These techniques were costly and could only boost compressive strength by a maximum of 40% [32]. However, processing rubber using quarry

dust (WQD) such as ceramic powder (CPW), which is considered waste, is much better among the previously mentioned processing methods, as the loss of strength was much lower than the previously used technique [35]. The success of the WQD pretreatment of rubber particles is ascribed to the treatment material particles' adherence to the rubber, which enhanced the rubber's ability to repel water [36].

Cement kiln dust (CKD) is a byproduct of the production of cement. The material under examination is a fine, powdery substance that resembles Portland cement. The substance under scrutiny is constituted of fine particles on a micron scale taken from electrostatic precipitators during the cement clinker manufacturing process. Aluminum, calcium, iron, magnesium, potassium, silica, sodium, and titanium are some of the most crucial components in chronic kidney disease. Additionally, manganese, sulfur, and chloride are among the chemical components of CKD bulk ingredients [37]. It is expected that the cement manufacturing sector in America produces about 15 million tons of CKD on an annual basis [38]. A medium-sized cement mill might generate up to 30,000 tons of CKD every year. Usually, these quantities are not recycled during production or used in any other way. A survey encompassing 60% of cement production facilities in the United States revealed that, owing to the elevated alkali content, substantial quantities of cement kiln dust are unfit for recycling [38].

CKD has a pH of almost 12, making it a very alkaline substance. Its sodium and potassium hydroxides speed up the blended slag cement's increase in compressive strength by breaking down the slag's glassy phase [39]. Cement kiln dust has the same fine-grained components as Portland clinker, but in different amounts. The range of its specific surface area is 4000–14,000 cm^2/g. Important elements of CKD include carbonates and chlorides, which are used as active agents in accelerating admixtures. Additionally, cement pastes that contain CKD are relatively less porous [40–42]. Using CKD in concrete manufacturing makes it possible to reduce the associated environmental effect and construction cost [40,41,43–46].

Eggshell waste (ESW) is categorized as trash or by-products from hatcheries and the food industry, and the majority of it is dumped in landfills untreated. In conventional concrete, ESW has been studied as a partial cement alternative; 5–15% substitutions have shown promising results [47], with a 5% substitution optimizing strength beyond control material qualities and demonstrating its viability in improving concrete properties. ESW exhibits resilience and a washable surface while reducing alkali-silica and sulphate expansions [47].

Polyvinyl alcohol fibers (PVA), polypropylene fibers (PPF), and polyethylene fibers (PE) are examples of fibers that are currently utilized in ECC. Synthetic fibers are a class of artificial polymeric fibers that are produced chemically. Steel and other synthetic fibers have been produced (S_tF) and carbon fibers (CF) are more prevalent in traditional concrete. Because of their low cost, the abundance of mineral resources in the Earth's crust, and minimal environmental impact, basalt fibers (BF) are popular [5,48]. Although PPF-ECC has a lower tensile strength than PVA-ECC, comparable levels of tensile ductility are seen when comparing the two materials [49–51]. PPF may be a desirable alternative to PVA in several applications due to its inexpensive cost and strong chemical stability [5]. PPF was added to standard concrete to improve its mechanical properties, including its compressive strength, split tensile strength, and flexural strength. But a high fiber content severely impairs the concrete's workability, durability, and compressive strength [52–54].

There is limited study on the application of ESW and CKD in cementitious products. To protect the environment, the need to recycle industrial by-products is increasing, this requires providing technical data on the performance of concrete and mortar containing CKD. The goal of this project was to create an environmentally friendly ECC by partially substituting different waste materials for cement and sand. In doses of 10% and 20%, CKD,

CPW, and ESW were utilized as partial cement substitutes. In doses of 25, 50, 75, and 100%, CR was utilized as a partial replacement for sand. Physical treatment using the same cement substitution materials (CKD, CP, ESP), and chemical treatment using sodium hydroxide, sodium silicate, and mix of sodium hydroxide and sodium silicate were carried out for the CR in the production of the proposed ECC. The effect of fiber types—such as S_tF, PPF, and BF—on the performance of ECC was also investigated.

2. Experimental Procedures

2.1. Materials

Portland cement (CEM I 52.5 N), ground granulated blast furnace slag (GGBFS), and silica fume (SF) with relative gravities of 3.15, 2.8, and 2.2, respectively, were combined with all ECC mixes in this study. The fine aggregate utilized was natural sand, which had a bulk density of 1.78 t/m^3, a specific gravity of 2.55, a particle size range of 0.125 to 4 mm, and a water absorption capacity rate of 0.8%. The sand volume was partially replaced with CR crumbs with a specific density of 0.97 at 25%, 50%, 75%, and 100%. Additionally, rubber surface treatment employing waste materials such as CKD, CPW, and ESP with specific gravities of 2.5, 2.2, and 2.8, respectively, was combined with rubber treatment using sodium hydroxide (NaOH) and sodium silicate (Na_2SiO_3). Additionally, at 10% and 20% volume, the three materials—CKD, CPW, and ESP—were utilized as partial cement substitutes. Particles smaller than 90 microns passed through sieve number 170. The particle size analysis is shown in Table 1. CR's specific gravity was 0.97, its apparent density was 0.53 t/m^3, and its particle size ranged from 2 to 5 mm. The sieve analysis of rubber and sand is shown as a potential replacement in Figure 1. All ECC mixes contained PPF with a diameter of 0.9 mm and a length of 12 mm. To compare the performance of CR-ECC with fibers commonly used as concrete additives, S_tF and BF were used in some concrete mixes, see Figure 2. The sieve analyses of cement, ESW, CPW and CKD are shown in Figure 3. The characteristics of the fibers utilized, as supplied by the manufacturers, are displayed in Table 2. A polycarboxylate ether-based superplasticizer (SP) was used at a rate of 10 kg/m^3 to make ECC more feasible.

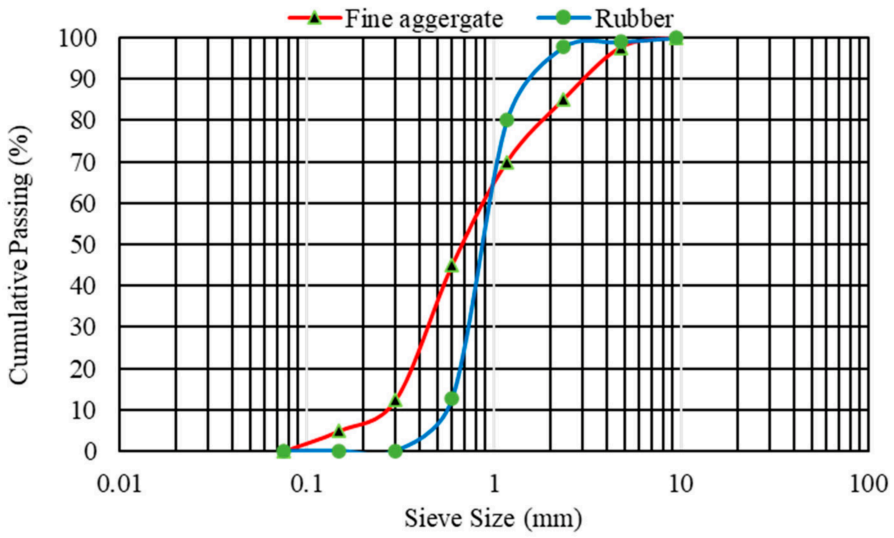

Figure 1. Sand and crumb rubber particle size distribution.



Figure 2. Fiber used for producing ECC mixtures, (**a**) PPF, (**b**) BF and (**c**) S_tF.

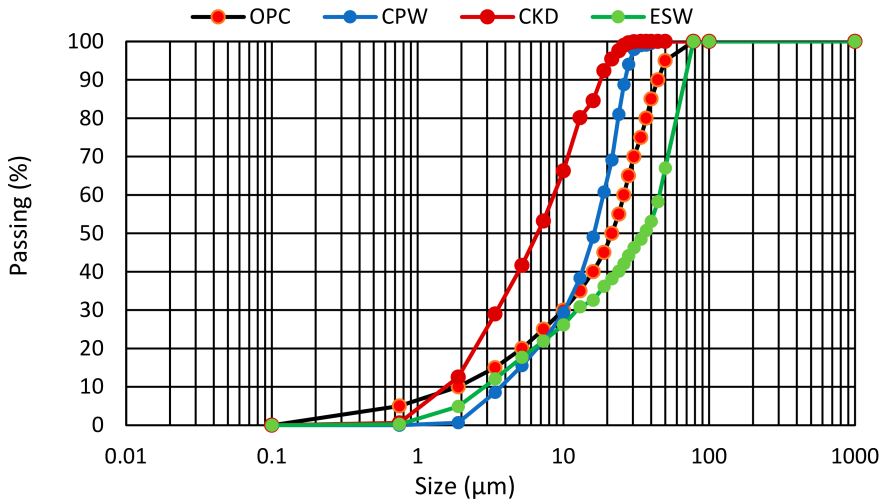

Figure 3. Cement particle size distribution, ESW, CPW and CKD.

Table 1. Particle size analysis.

Material	Cement Kiln Dust (CKD)	Ceramic Powder (CP)	Eggshell (ESP)
Average particle size (d_{50})	6.659 microns	19.45 microns	38.78 microns
Total particle size (d_{98})	24.18 microns	85.02 microns	98.25 microns
Specific surface	497.4 kg/m^2	196.4 kg/m^2	218.4 kg/m^2

Table 2. Dimensions and mechanical properties of fibers.

Fiber Type	Length (mm)	Diameter (mm)	Density (gm/cm^3)	Tensile Strength (MPa)	Elastic Modulus (GPa)	Elongation at Break %
Polypropylene fiber	12	0.034	0.91	400	3.75	200
Steel fiber	12	0.8	7.85	1300	210	
Basalt fiber	12	0.015	2.65	2600	85	2.9

Although ceramic powder waste (CPW) and eggshell waste (ESW) exhibit certain pozzolanic characteristics due to their silica and calcium oxide contents, cement kiln dust (CKD) cannot be strictly classified as a pozzolanic material. CKD typically consists mainly of calcium carbonate ($CaCO_3$), partially calcined raw materials, and significant amounts of alkali compounds. Therefore, its contribution to strength development is primarily attributed to its micro-filler effect, which improves particle packing and matrix densification.

In addition, the high alkalinity of CKD may chemically stimulate the hydration reactions of other reactive components in the system, acting as an alkaline activator rather than a direct pozzolanic reactant. Consequently, the role of CKD in the composite system should be interpreted mainly through physical filling and chemical excitation mechanisms rather than secondary pozzolanic hydration.

2.2. Mixing Proportion

Table 3 provides the details of the 19 ECC mixes that were prepared for the current study. The control ECC mixture (CC) was created using the total weight of the cementitious material, including cement, SF, and GGBFS, is 1231 kg/m^3. For all mixes, the proportion of SF to GGBFS was maintained at 20% and 60% of the cement weight, respectively. CR mixes were made by substituting rubber for a portion of the sand volume at a rate of 25% (NTR25), 50% (NTR50), 75% (NTR75), and 100% (NTR100). At 50% rubber content, chemical treatment of rubber using sodium hydroxide (TR NaOH), sodium silicate (TR Na_2SiO_3), and sodium silicate plus sodium hydroxide (TR NaOH/Na_2SiO_3), as well as physical treatment of rubber was performed using ESW, CPW, and CKD in (TR ESW), (TR CPW), and (TR CKD) blends, respectively. The CKD method of rubber particle pre-treatment was chosen in accordance with the prevised study, as an option that could potentially improving the performance of TCR-ECC and using BF (TR CKD-BF) and S_tF (TR CKD-S_tF) at same volume of 2% to compare with PPF. Cement volume was partially replaced at rates of 10% and 20% using three types of materials: ESW (TR-10 ESW, TR-20 ESW), CKD (TR-10 CDK, TR-20 CDK), and CPW (TR-10 CPW, TR-20 CPW). In the concrete mixtures, a water/binder (w/b) ratio of 0.27 was upheld, incorporating a superplasticizer (SP) at 10 kg/m^3 and 2% polypropylene fibers (PPF) in all mixtures.

Table 3. Design of ECC mixes per 1 m^3.

NU.	Groups	Mix Code	Cement (kg)	GGBFS (kg)	SF (kg)	Sand (kg)	CR (kg)	CKD (kg)	CPW (kg)	ESP (kg)	Water (kg)	SP (kg)	BF (kg)	S_tF (kg)	PPF (kg)
1	Control mix ECC	CC	685	410	136	548	-	-	-	-	332	10	-	-	25
2	Non-treated CR replaced sand	NTR25	685	410	136	411	50.14	-	-	-	332	10	-	-	25
3		NTR50	685	410	136	274	100	-	-	-	332	10	-	-	25
4		NTR75	685	410	136	137	150.4	-	-	-	332	10	-	-	25
5		NTR100	685	410	136	-	200.5	-	-	-	332	10	-	-	25
6	CR treated using NaOH	TR NaOH	685	410	136	274	100	-	-	-	332	10	-	-	25
7	CR treated using Na_2SiO_3	TR Na_2SiO_3	685	410	136	274	100	-	-	-	332	10	-	-	25
8	CR treated using NaOH/Na_2SiO_3	TR NaOH/ Na_2SiO_3	685	410	136	274	100	-	-	-	332	10	-	-	25
9	CR treated using ESW	TR ESW	685	410	136	274	100	-	-	-	332	10	-	-	25
10	CR treated using CPW	TR CPW	685	410	136	274	100	-	-	-	332	10	-	-	25
11	CR treated using CKD	TR CKD	685	410	136	274	100	-	-	-	332	10	-	-	25
12	CR treated using CKD, with BF	TR CKD-BF	685	410	136	274	100	-	-	-	332	10	70	-	-
13	CR treated using CKD, with S_tF	TR CKD-S_tF	685	410	136	274	100	-	-	-	332	10	-	210	-
14	CR treated using CKD, with ESW replaced cement	TR-10 ESW	616	410	136	274	100	-	-	57	332	10	-	-	25
15		TR-20 ESW	548	410	136	274	100	-	-	110	332	10	-	-	25
16	CR treated using CKD, with CDK replaced cement	TR-10 CDK	616	410	136	274	100	57	-	-	332	10	-	-	25
17		TR-20 CDK	548	410	136	274	100	110	-	-	332	10	-	-	25
18	CR treated using CKD, with CPW replaced cement	TR-10 CPW	616	410	136	274	100	-	50	-	332	10	-	-	25
19		TR-20 CPW	548	410	136	274	100	-	98	-	332	10	-	-	25

GGBFS = ground granulated blast furnace slag, SF = Silica fume, CR = Crumb rubber, CKD = cement kiln dust, CPW = ceramic powder, ESP = eggshell waste, SP = Superplasticizer, PPF = polypropylene fibers, S_tF = steel fibers, BF = basalt fibers.

The replacement ratios of CR, CKD, ESW, and CPW were chosen using a mixture of earlier research and initial laboratory testing. Low replacement levels (10% of cement for CKD, ESW, or CPW) were chosen to evaluate initial effects on workability, mechanical performance, and durability without significantly altering the matrix. For CR, higher replacement levels (50–100% of sand) were selected to investigate the maximum feasible incorporation and its influence on ECC properties. Previous studies have either only partially substituted sand or used untreated rubber, leaving a knowledge gap regarding the overall performance of ECC mixtures with treated CR at high replacement levels. Therefore, the selected ratios allow a systematic assessment of each material's contribution while addressing this research gap.

2.3. Treatment Methods

CR, obtained from waste tires, poses considerable difficulties when incorporated into cementitious materials, chiefly because of its hydrophobic characteristics and inadequate adhesion with cement. Concrete's mechanical qualities may be adversely affected by surface treatment with CR particles, increasing brittleness and decreasing compressive strength. Previous studies [55,56] indicate that the weak interaction between crumb rubber (CR) and the cementitious matrix is mainly attributed to the non-polar surface properties of CR, which hinder the formation of a strong interfacial bond with the surrounding cement paste. Consequently, it is imperative to process CR to mitigate these common problems and improve its suitability for cementitious materials.

In this study, six treatment methods were applied to crumb rubber (CR) particles (NaOH, Na_2SiO_3, NaOH/Na_2SiO_3, ESW, CPW, and CKD) to enhance the compatibility between the rubber particles and the cementitious matrix, as illustrated in Figure 4. In order to successfully incorporate CR into ECC, this treatment was necessary to reduce the materials' negative environmental effects while maintaining or improving the compound's performance.

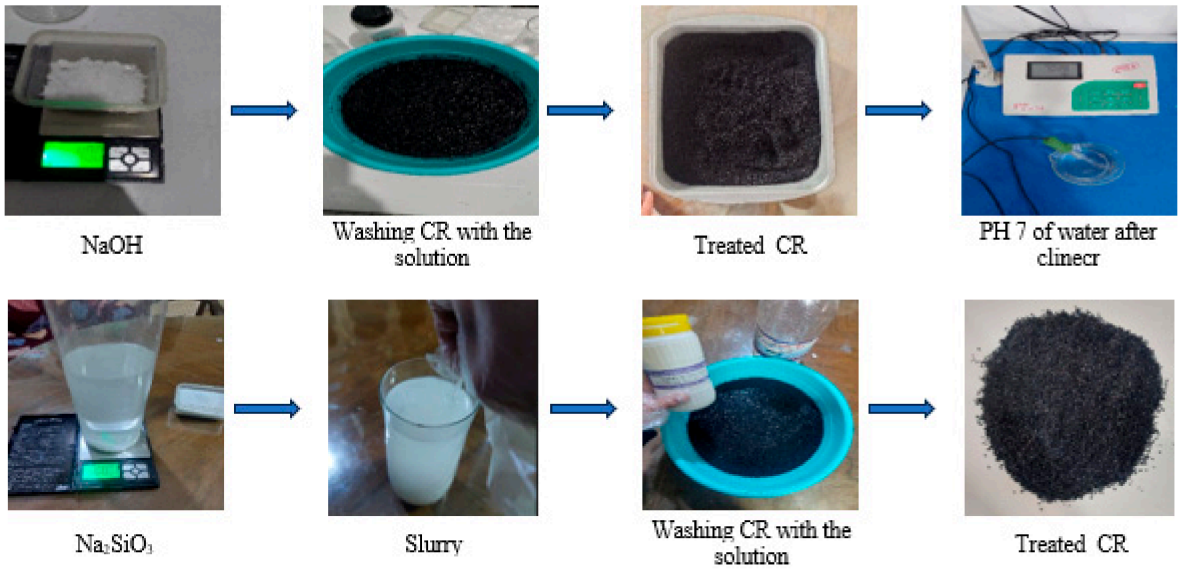

Figure 4. *Cont.*

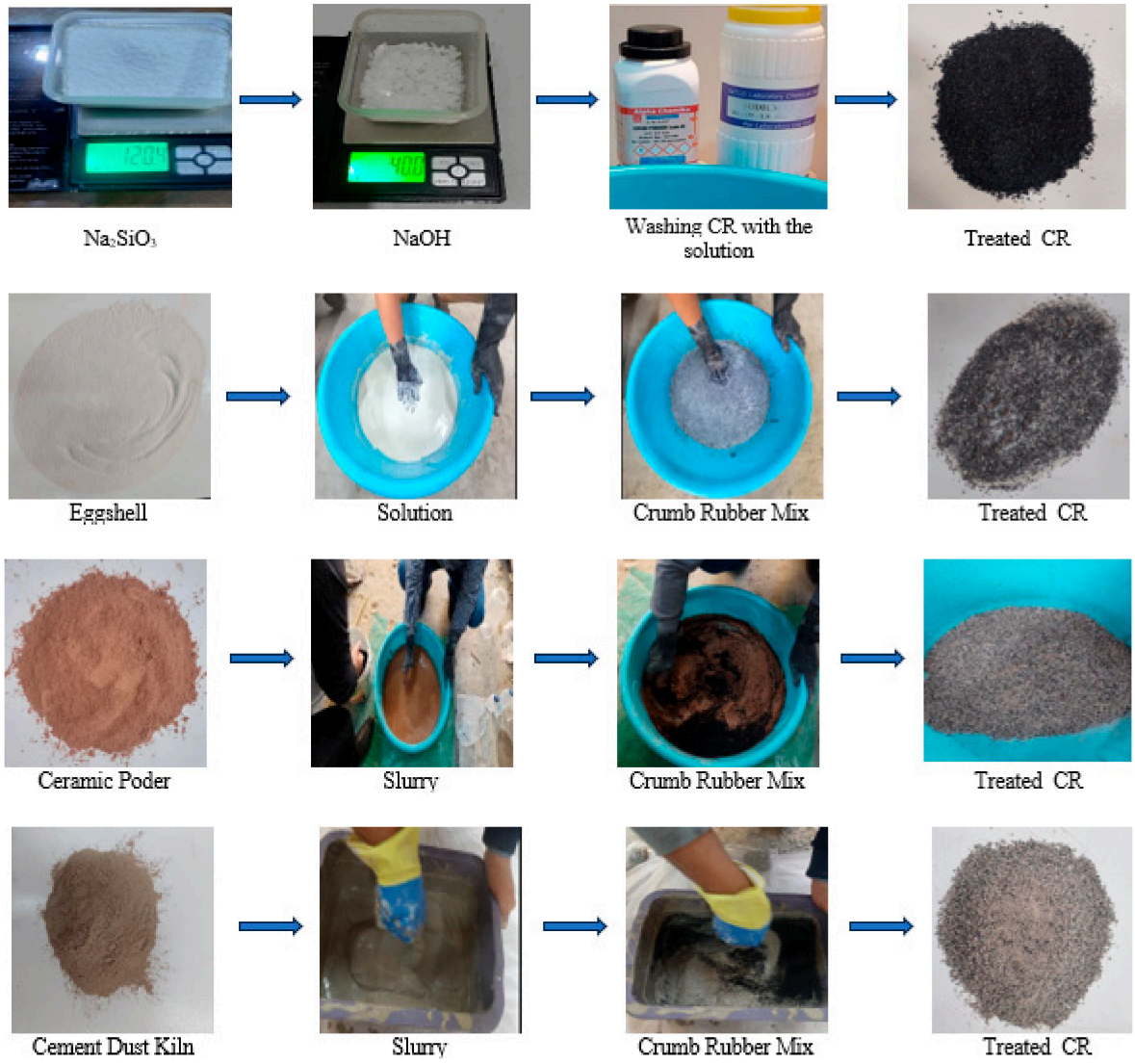

Figure 4. Treatment of rubber crumbs using physical and chemical processing techniques.

2.3.1. Chemical Method

The chemical treatment method included CR treatment using NaOH and/or Na_2SiO_3. Utilizing NaOH flakes and distilled water, a 10% NaOH solution was made in a glass flask. A glass rod was then used to stir the mixture. The rubber was then progressively added to the mixture while being stirred until it was completely submerged. The treated rubber was allowed to air dry after being left at room temperature for 30 min and then rinsed with tap water until a neutral pH (≈7) was reached. The rubber particles that had been treated were then kept in plastic bags until they were added to the ECC mixes. In another chemical treatment method, CR particles were submerged in a 10% sodium silicate was solution made with distilled water and left for half an hour at room temperature. After being treated with Na_2SiO_3, the rubber particles were cleaned with tap water and left to dry at room temperature. After treatment, the rubber was put in plastic bags until it was used in ECC mixtures.

The third chemical treatment procedure involved mixing solutions of sodium hydroxide (NaOH) and sodium silicate (Na_2SiO_3). First, a 10% NaOH solution was made and allowed to sit at room temperature for half an hour. After that, it was combined with the sodium silicate solution for another half hour using a mechanical mixer. After that, the rubber crumbs were submerged in the mixture for half an hour. The solution had a Na_2SiO_3/NaOH ratio of 3.0.

2.3.2. Physical Method

Slurries were made using water-to-waste material ratios of 0.7, 0.5, and 0.7 by weight for ESW, CPW, and CKD, respectively, in the physical treatment procedure. These ratios were chosen to provide uniform particle dispersion and slurry viscosity. After being submerged in the slurry and stirred for five to ten minutes, the CR particles were taken out. As shown in Figure 4, the treated particles were then put on plastic plates and left to dry for a full day at room temperature. Uniformity was vital for ensuring consistent application throughout all the rubber particles.

2.4. Procedures for Preparing and Testing Specimens

2.4.1. Workability and Mechanical Properties

The mini-slump test is regarded as a quick and economical method for ECC. According to AS 1012.3.5, a downscaled cone was used in this study's mini-slump test setup [49]. The mini-slump cone, with specifications of 116 mm in height and 38 mm and 76 mm for the upper and lower diameters, respectively, is illustrated in Figure 5. According to the BS EN 12390 standard, compressive strength tests were performed [50,56] using concrete cubes measuring 50 × 50 × 50 mm, assessed at 7, 28, 56, 120, and 180 days. To analyze the tensile stress–strain behavior of each mixture, dog-bone specimens were employed, in line with recommendations from the Japan Society of Civil Engineering [57]. Dog bone samples used in the uniaxial tensile test are shown in Figure 6 along with their dimensions. The loading was done at a constant rate of 0.3 mm/min. As shown in Figure 7, plate specimens of 300 × 100 × 15 mm were prepared for the flexural strength assessment. After 28 days, they were exposed to a 4-point bending load at a loading rate of 0.5 mm/min.



Figure 5. Mini slump test of ECC.

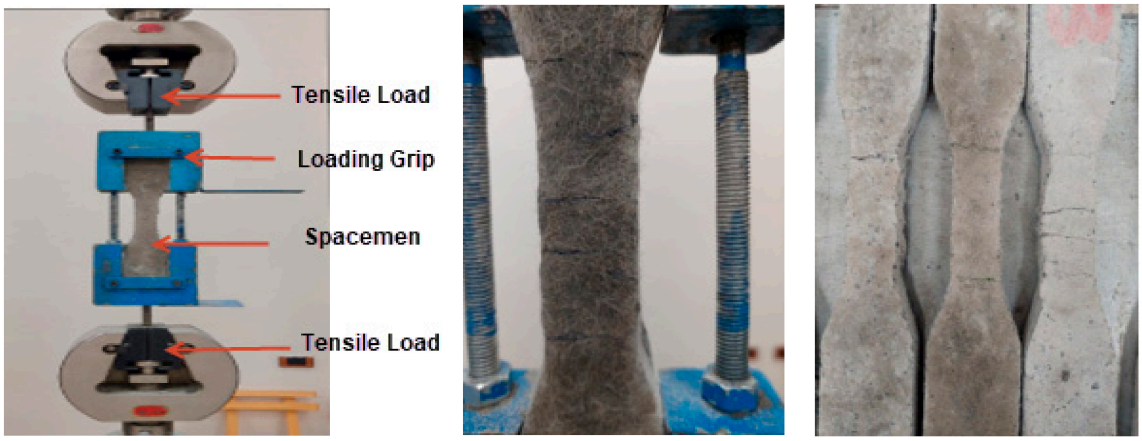

Figure 6. Uniaxial tensile test of ECC.

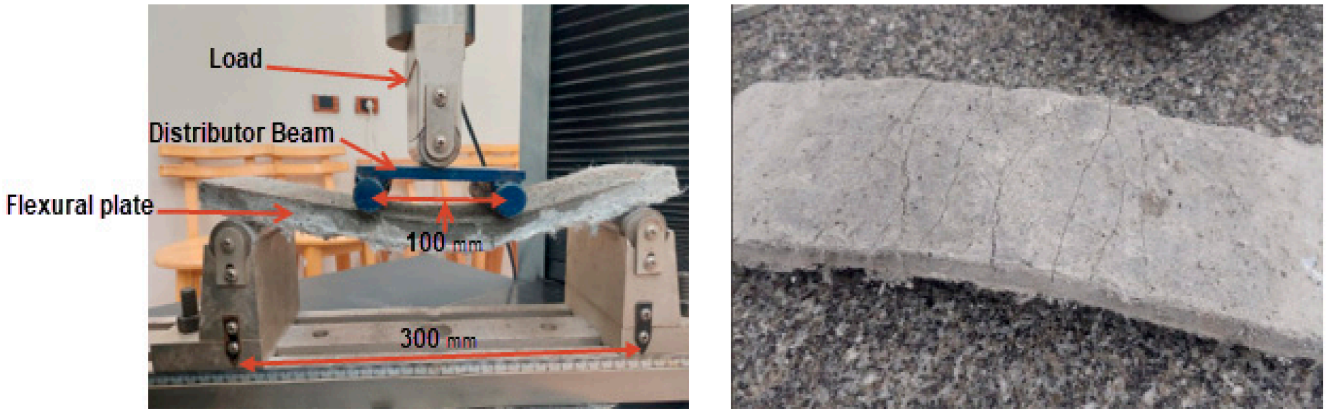

Figure 7. Flexural strength test of ECC.

2.4.2. Sorptivity

Through the concrete's resistance to permeability, including aggressive solutions, its durability was determined [58]. Water absorption of mixtures is a durability test that evaluates their resistance to the penetration of solutions that are aggressive in the matrix. The absorption test examines mass increase over time due to water absorption. This occurs when a sample's capillary action exposes one of its surfaces to water (Figure 8).

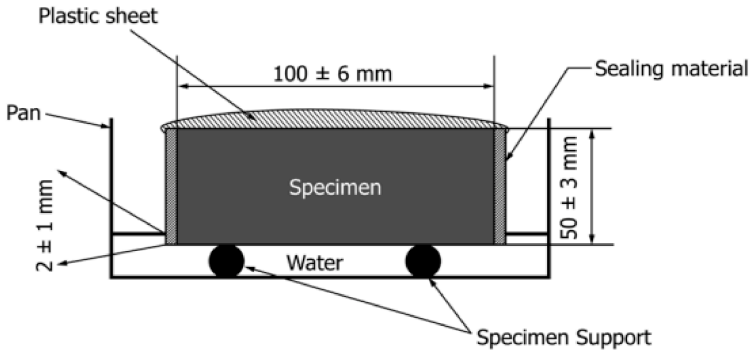

(**a**)



(**1**) ECC disk Drying. (**2**) ECC disk sealing. (**3**) ECC sorptivity testing.

(**b**)

Figure 8. (**a**) Sorptivity test setup. (**b**) Preparation of ECC specimens for sorptivity test.

ASTM C1585-13ST [59] cylindrical samples measuring 100 mm in diameter and 50 mm in thickness were assessed for absorption (see Figure 8a). After being water-treated for 28 days, the samples were dried for three days at a temperature of 50 ± 2 °C and a

humidity rate of 80 ± 3% until their weight remained constant. Before the absorption test, the specimens' lateral surfaces were covered with duct tape and their top surfaces were sealed with a plastic sheet fastened with elastic bands. Consequently, the movement of water was permitted exclusively upright through the bottom surface.

The experiment comprised two plastic bars, that were situated in a plastic container. The water level was sustained at 3 mm. The measurements were taken at a point 1 mm above the bottom surface of the specimens—see Figure 8b. Ref. [56]—at 1, 5, 10, 20, 30, and 60 min. and after every hour up to 6 h. Finally, every 24 h for eight days. The dry weight was recorded before being submerged in water, and then the weight was taken at the intervals specified by the ASTM 1585.13 standard [60]: at 1, 5, 10, 20, 30, and 60 min. and after every hour up to 6 h. Finally, every 24 h for eight days. The weight of the specimens was measured using an electronic balance. This was accomplished after the surplus surface water was removed using a damp towel. The specimens were thereafter returned to the container within 15 s for the subsequent interval measurements. During the course of the experimental procedure the water height was 2 ± 1 mm from the level of the bottom surface of the sample. The relationship between the cumulative absorbed water volume per unit surface area (I) in units of (mm^3/mm^2) and the square root of time was plotted. I was determined using Equation (1) according to the ASTM C1585-13 standard [60] as below:

$$I = \frac{M_t}{Ad} \tag{1}$$

where d represents the density of water (g/mm^3), A is the surface area of the lowest portion of the sample exposed to water (mm^2), and M_t is the change in the sample's mass (gm) at a specific period (t). The absorption coefficients were calculated using the slope of the best-fit line for I plotted against the square root of time. By the following equation:

$$I = S\sqrt{t} + b \tag{2}$$

where the sorptivity coefficient ($mm/s^{0.5}$) is used to define absorption rate S. The constant number b, which correlates to the observed time t in seconds, explains the impact of initial water filling at the concrete surface.

According to ASTM C1585-13 [60] capillary absorption goes through two stages, the first being from 0 to 6 h.—called the initial absorption stage. After the beginning of the test and the final phase, which is absorption that extends from 6 h to 8 days in this study, the data obtained from the two phases were entered to calculate the primary and secondary absorption coefficients. Additionally, to make sure it reached the minimum required value of 0.98, the correlation coefficient (R2) was utilized.

2.4.3. Microstructural Analyses

A JEOL JSM 6510 LV scanning electron microscope at an acceleration voltage of 30 kilovolts was employed. After 56 days, the ECC sample's surface morphology and microstructure were examined and described. After that, the samples were coated with a 12-nanometer-thick layer of gold before being examined. SEM analysis was done on the control sample mixture, and the analysis also included some mixtures containing 50% rubber for comparison (NTR50, TR CKD, TR CKD-BF, and TR CKD-S_tF), to carefully evaluate the impact of the applied treatment techniques on the rubber. An energy-dispersive X-ray spectrometer (EDX) (Oxford X-Max 20) was employed to determine each element's atomic percentage in the standard mixtures.

3. Results and Discussion

3.1. Workability

Figure 9a illustrates the results pertaining to the workability of ECC mixtures that contained rubber crumbs. In ECC concrete mixtures including untreated rubber, the slump value dropped as the rubber replacement ratio for fine particles increased. The results revealed that the slump values decreased by 13%, 30%, 35%, and 50% at sand replacement ratios of 25%, 50%, 75%, and 100%, respectively, relative to the control mix. This reduction is attributed to the untreated rubber fragments containing contaminants on their outside surfaces, which increase water requirements. The existence of crumb rubber in ECC mixtures results in diminished workability, attributable to the hydrophobic characteristics of rubber, inadequate particle gradation, and the porosity of the concrete relative to traditional ECC mixtures. Rubber also has an irregular shape, slightly serrated edges, and a rough texture, unlike the natural shape of sand, which adds to this appearance.

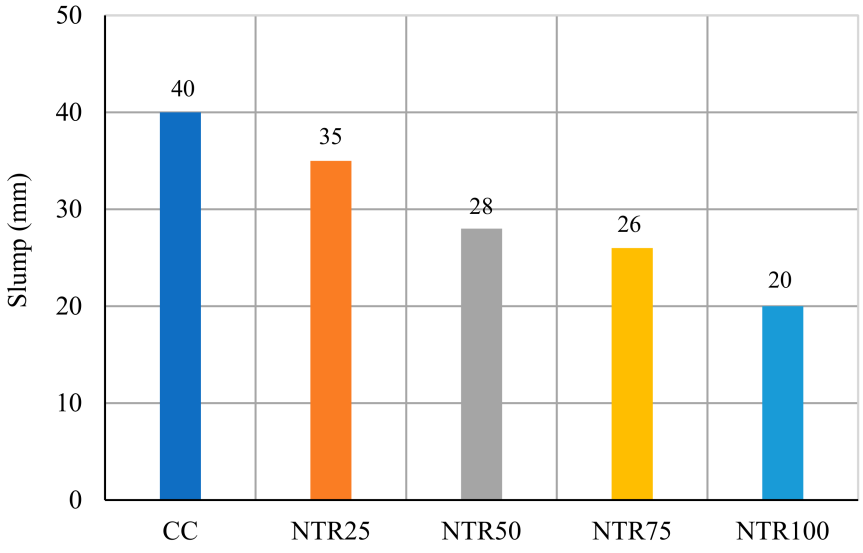

(**a**)

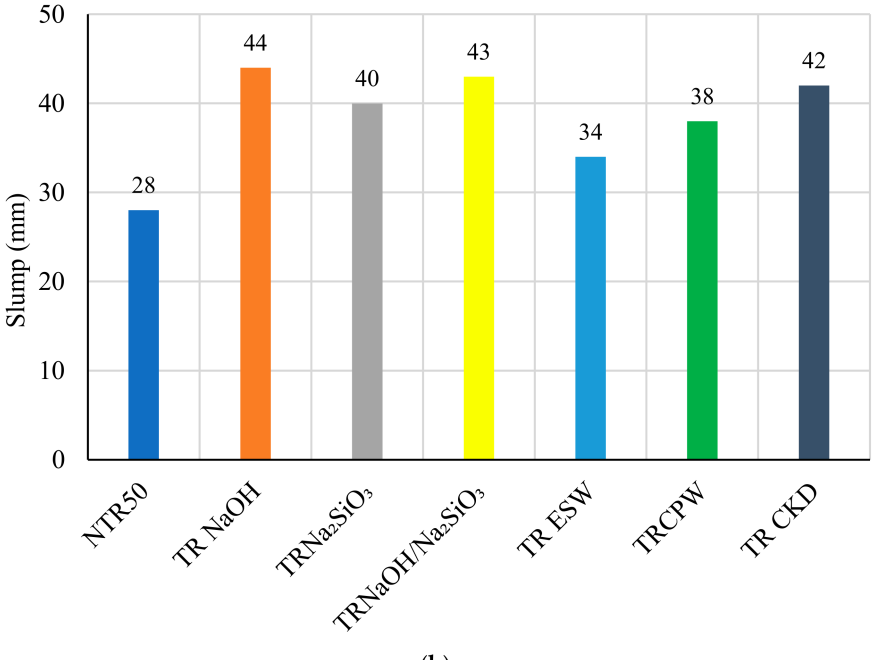

(**b**)

Figure 9. *Cont.*

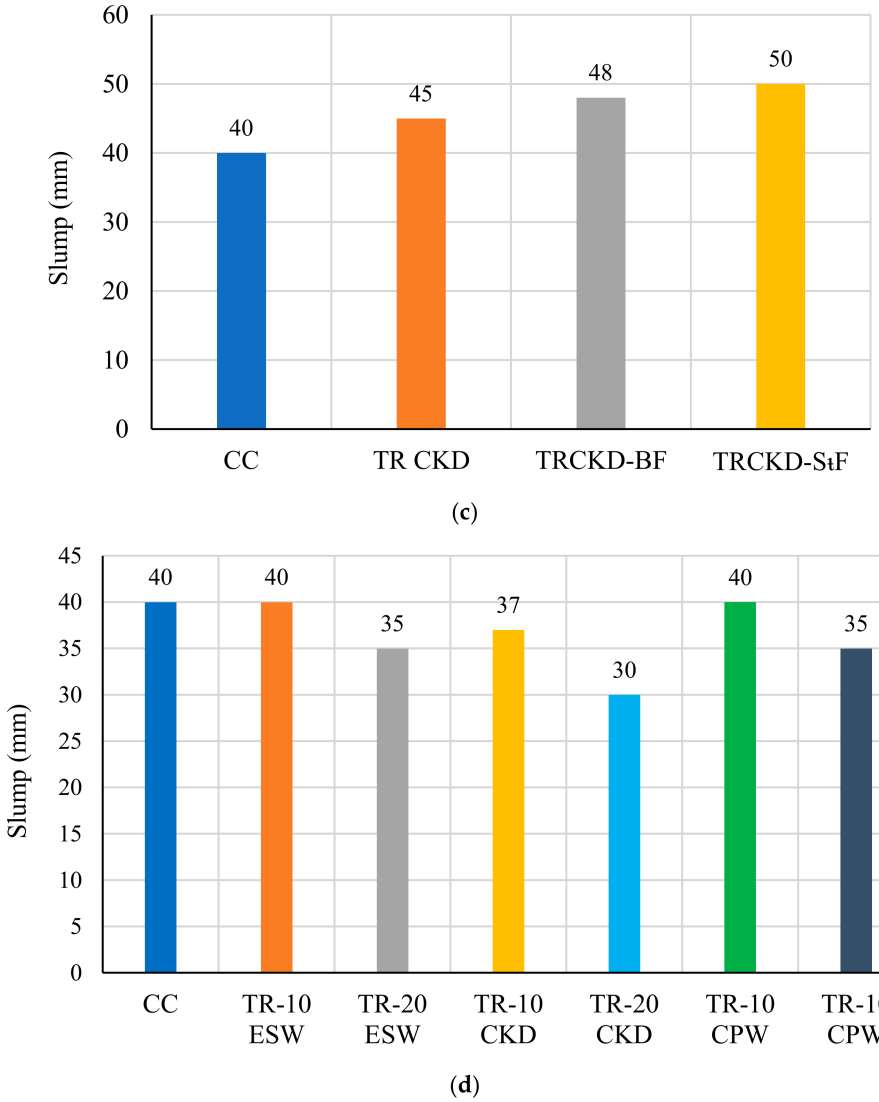

Figure 9. (**a**) Measured slump values of ECC made with different crumb rubber contents. (**b**) Measured slump values of ECC with different crumb rubber treatments. (**c**) Measured slump values of ECC with different types of fiber. (**d**) Measured slump values of ECC with treated rubber and partial cement replacement.

As shown in Figure 9b, a substantial improvement in workability was observed for chemically treated samples at a 50% rubber replacement ratio. Specifically, the slump value for the mixture incorporating sodium hydroxide and sodium silicate treatments increased by 57%, indicating the highest operational performance among all tested samples. This enhancement was notably superior when compared to the mixture containing untreated rubber at the equivalent replacement level.

The mix's workability is enhanced by sodium silicate's lubricating effect, while the use of NaOH improves surface roughness, leading to better enhanced adherence with the cement paste. Ewan et al. [61] reported that NaOH reacts with rubber particles due to the presence of a zinc stearate layer on their surface. This layer is responsible for the hydrophobic nature of the rubber. The reaction converts zinc stearate into soluble sodium stearate, which can be removed by washing with tap water, thereby reducing the hydrophobicity of the rubber crumbs. Furthermore, the Na^+ ions from the treatment solution can replace the H^+ ions from the acidic carboxyl groups on the surface of the rubber crumbs, forming of a fundamental layer surrounding the rubber particles is pivotal in impeding deleterious interactions between the acidic carboxyl groups and alkaline

hydration products [61]. However, the NaOH treatment did not demonstrate any capability to overcome the issue of voids.

As illustrated in Figure 9b, ECC mixtures incorporating physically treated rubber crumbs demonstrated a significant enhancement of workability relative to the control sample. The treated rubber tire crumbs' (TCR) smaller particle size is the main reason for this improvement compared to the coarser untreated rubber, as well as the increased air entrainment observed on the surface of untreated rubber, which contributed to the reduction in slump. Notably, the reduction in slump spread was less substantial in the TRESW sample; however, the application of eggshell-based treatment led to a 21% increase in workability. Furthermore, in mixtures containing TRCPW and TRCKD, compared to the mixes that use untreated rubber with a 50% replacement rate, the slump values improved by 0.35% for the mix treated with TRCPW and by 50% for the mix treated with TRCKD. These results indicate an improvement in the soft properties of the ECC mix after physical treatment.

In terms of the influence of adding steel fibers and basalt fibers instead of polypropylene fibers, as shown in Figure 9c, it can be observed that the mixture containing BF had lower workability compared to the S_tF mixture by 14% and 19%, respectively, compared to the polypropylene fibers mixture. This causes difficulties in the movement of the concrete, making the mixture more cohesive. The effect of BF on slump was less significant than the effects of steel fibers due to the relatively smaller aspect ratio and the flexibility of the fibers used, which can reduce this slump reduction.

The increased water absorption rate is responsible for the decrease in slumps. This is a property of the PPF dosage, resulting in a lower amount of free water within the concrete matrix. Moreover, the consumption of available cementitious materials due to the relatively large surface area of BF reduces the lubrication within the concrete matrix. Sadrmomtazi [52] mentioned that high doses of BF have a negative effect during mixing and placing the mortar.

In comparison to the mixture produced with untreated rubber at the same replacement ratio, the workability of the ECC mixture with crumb rubber at a 50% sand replacement ratio treated with Na_2SiO_3, NaOH/Na_2SiO_3, and NaOH improved by 28%, 42%, and 57%, respectively. There was a gradual increase in the combined water content up to 2.5% as the CKD increases. The presence of alkalis, chlorides, and sulfates in the CKD, along with hydrated lime, is the reason for the activation of GBFS. As the CKD reaches 10% and 20%, the combined water content reduces compared to the control mixture. This is shown in Figure 9d. This is primarily due to the decrease in OPC, which is itself a result of the rise in cement dust. Therefore, the phases of OPC decreased, including C3S, β C2S, C3A, and C4AF. And for the hydraulic properties of these phases, the significant Impact is on the chemically bound water [62].

3.2. Compressive Strength

Compressive strength tests were conducted on all mixes at 7, 28, and 56 days after curing. As illustrated in Figure 10, the compressive strength gradually decreased as the CR content was increased in substitution of fine aggregate. For sand replacement ratios of 25%, 50%, 75%, and 100%, the compressive strength dropped by 5.6%, 24.3%, 60%, and 62.8% at 28 days. The mixture with 100% replacement of rubber for sand had the lowest observed compressive strength of 26 Mpa.

Compared to natural sand, the hardness of CR caused a noticeable decrease in compressive strength, accompanied by a higher CR rate in the mix, in addition to the potential development of a weaker interfacial transition zone between the CR particles and the surrounding cementitious matrix. Furthermore, studies have shown that the number of closed pores increases within the matrix with the incorporation of CR—it is likely that

the compressive strength reduction is due to this. These findings are consistent with previous studies involving the utilization of CR as an aggregate in conventional concrete mixes [47,48]. Despite this, Figure 10a demonstrates that all CR-ECC mixes investigated maintained compressive strengths above 24 Mpa, indicating their suitability for various structural applications.

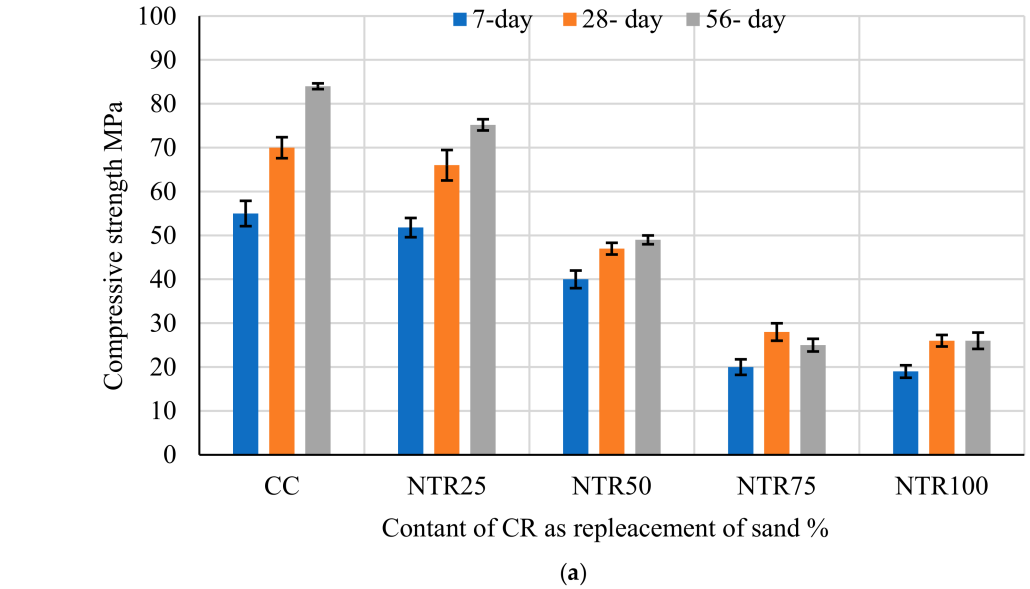

(**a**)

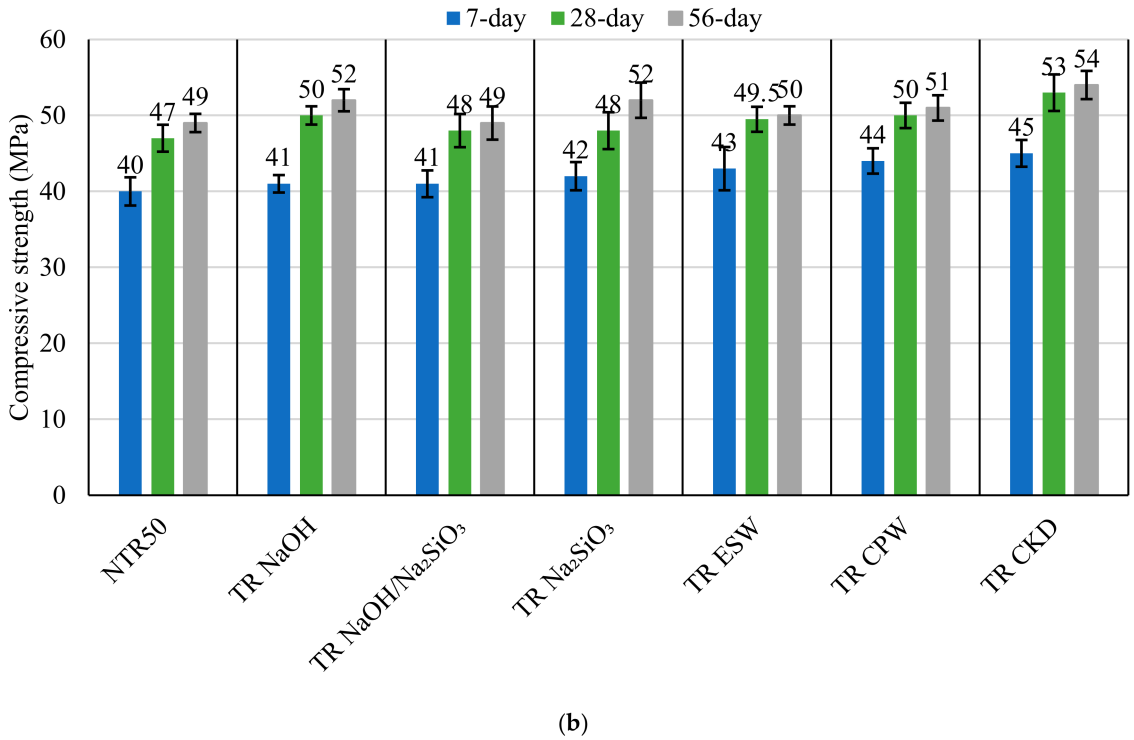

(**b**)

Figure 10. *Cont.*

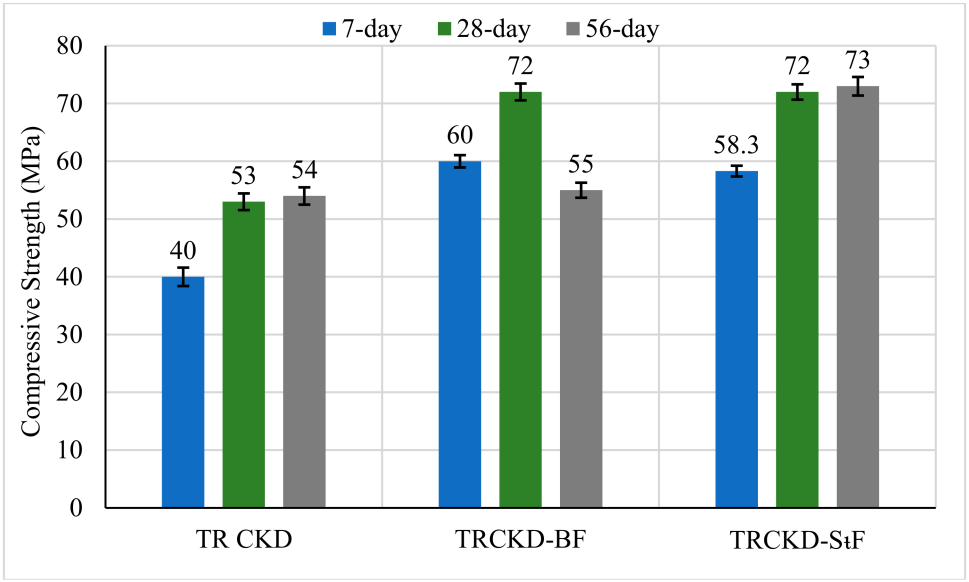

(**c**)

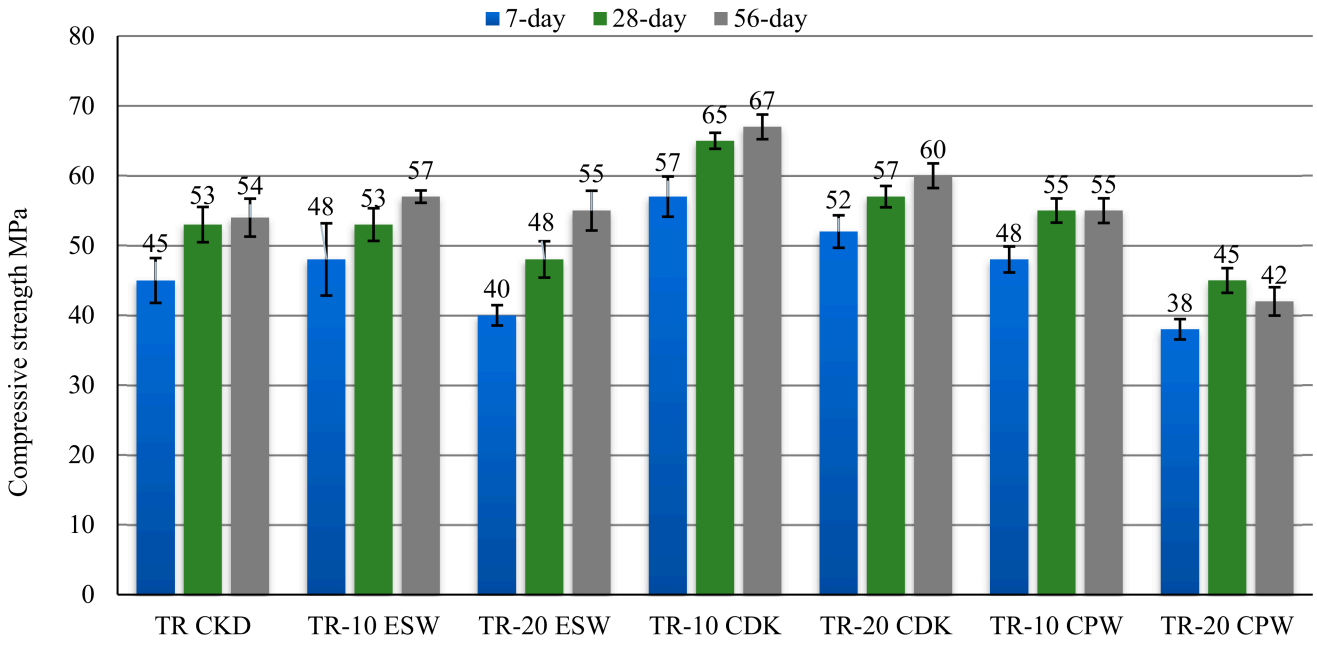

(**d**)

Figure 10. (**a**) Effect of CR content on compressive strength. (**b**) Effect of rubber treatment on ECC compressive strength. (**c**) Effect of different types of fiber on ECC compressive strength. (**d**) Effect of cement replacement on ECC compressive strength.

Chemical treatment of CR was conducted using NaOH, Na_2SiO_3, and NaOH/Na_2SiO_3. Meanwhile, TR NaOH exhibited the greatest strength at all of the chemically treated ages for TRECC specimens. TR Na_2SiO_3 exhibited the lowest compressive strength. Enhancements in CRECC compressive strength were noted at 28 days, with increases of 7.5%, 3%, and 2.5% when chemically treated with NaOH, NaOH-Na_2SiO_3, and Na_2SiO_3, respectively, as illustrated in Figure 10b. Consequently, treatment with 10% NaOH is optimum for augmenting the compressive strength of the CR. Awan et al. [53] demonstrated that treatment with NaOH improved the rough texture of the rubber particles. Mohammadi et al. [55] showed that the zinc stearate layer present in rubber reacts with NaOH during processing, causing the rubber to become hydrophobic due to the sodium stearate produced from the reaction, which can be easily removed with water when washing the rubber because

it dissolves in water, thereby reducing its hydrophobicity. Additionally, the H^+ in the acidic carboxylic group on the surface of CR can replace Na^+ from the treatment solution, which stops the undesirable reaction between the acidic carboxylic group and the alkaline hydration products. Due to this, a basic layer surrounding CR is formed [54]. Nonetheless, the NaOH treatment did not overcome the issue of voids in the rubber particles.

On the other hand, significant improvements in the compressive strength of ECC were observed on days 7, 28, and 56 when 50% of the sand was replaced with physically treated CR. Specifically, enhancements of 12.5%, 15%, and 12.5% were recorded with CR treated using cement kiln dust (TRCKD); 10%, 7.5%, and 5% with CR treated using ceramic powder (TRCPW); and 7.5%, 1%, and 2% with CR treated using eggshell powder (TRESW), relative to the control CC mixture. These enhancements are attributed to the physical surface treatment, which modifies the hydrophobic properties of rubber to become more hydrophilic, particularly in the presence of waste, thereby strengthening the bond between the particles of the rubber and the cement matrix. Additionally, the treatment process helps regulate the porosity of the CR, further contributing to improved mechanical performance. As illustrated in Figure 10b, the use of physically treated CR with a 50% replacement rate of CR coating improves the cement's adherence to rubber.

Figure 10c presents the compressive strength results of ECC mixtures at 7 and 28 days. After 28 days, it is evident that the mixtures containing equal proportions of BF and S_tF, each constituting 2% of the ECC volume, exhibited higher compressive strength compared with the mix reinforced with PPF. In addition, a slight increase of about 3% in compressive strength was observed for the mixture incorporating BF and S_tF at a dosage of 0.35%. At 7 days, the results indicate that S_tF had a similar effect to BF on the compressive strength of ECC, showing comparable performance at both 7 and 28 days.

Upon comparison of the data after 56 days, it is evident that the ECC mix incorporating S_tF exhibits superior compressive strength relative to the other mixes, succeeded by those containing equivalent ratios of BF and PPF. This contradicts the observations made on compressive strength at 7 days. It is clear that there is a difference in compressive strength between the mixture containing S_tF and the one containing PPF attains 35%. This demonstrates the significant contribution of steel fibers to the enhancement of compressive strength.

As shown in Figure 10d, the compressive strength of ECC was significantly increased by replacing 10% of the cement with waste material, CKD, CPW, and ESW. In comparison to the TCR-ECC mixture, the compressive strength of ECC containing TR-10CKD rose by 26.6%, 22.2%, and 24% on days 7, 28, and 56, respectively. This improvement is due to the smaller particle size of CKD, which enhances the cohesion of the mixtures. When TR-10CPW was used, the corresponding increases were 6.5%, 3.7%, and 3.6% at the same time intervals, while TR-10ESW addition led to gains of 6.6%, 5.4%, and 5.5%, respectively. Both the chemical and physical contributions of waste are responsible for these improvements. Because there are fewer voids and more surfaces available, the fine particles of waste materials physically act as fine fillers between the cement grains, increasing the formation of calcium silicate hydrates (C–S–H), calcium hydroxide (CH), and other hydration products that improve the hydration process [63]. Chemically, the pozzolanic nature of CKD enables additional C–S–H formation through reactions with cement hydrates. Moreover, the particle morphology of CPW and ESW characterized by fine size, irregular shape, and rough texture not only increases filler effectiveness but also enhances the interfacial transition zone (ITZ) between the aggregates and the paste, thereby improving the overall composite structure [19].

Mixtures containing 20% CPW demonstrated reduced compressive strength. It was observed that with the increase in replacement content, there was a decrease in the compressive strength of the TR CKD mixture. A previous study [44] showed a decrease in

strength with an increase in the CPW ratio. The ceramic particles present in the ceramic powder deplete the C–S–H gel during hydration when cement is replaced with CPW. The pozzolanic property of CPW particles during hydration played a significant role in improving strength noticeably at early ages.

The compressive strength exhibited a minor reduction at 20% CKD as a partial substitute for cement. A decline in compressive strength typically refers to the diminished cement content, and higher porosity and advanced stages of the choro and sufflaminate phases enhance the softening and expansion of hydration products due to the high percentage of free lime in cement dust. Wang et al. [64] also investigated the impact CKD on the compressive strength of mortar over 28 days with a water/binder ratio of 0.50 and partial replacement ratios (0%, 15%, and 25%) of PC. When the replacement reaches 15% of cement with CKD, it leads to an increase in the compressive strength of the mixtures (47.8 MPa) compared to cement alone (46.3 Mpa); this is what the authors discovered. In addition to this, specifically at 25% CKD (39.4 Mpa), the compressive strength declined compared to the ordinary cement sample. Increasing the percentage of added cement kiln dust leads to a decrease in the compressive strength compared to the sample with the lower percentage, due to the reduction in the hydraulic properties of CKD. Wang et al. [64] assumed that the strength improves for the 15% ratio; it is attributed to an appropriate alkalinity level for the dissolution of silicates and the production of C–S–H.

According to Figure 10d, it is evident that the compressive strength began to rise at a 10% substitution of eggshell powder in comparison to the control mix design TR CKD. The compressive strength is enhanced by adding eggshell powder. The same effect has been observed—with the highest value reaching 57 megapascals after 65 days of treatment and the lowest value being 48 megapascals after 21 days of treatment. The compressive strength also improved on the twenty-eighth day compared to what it was on the twenty-first day during the curing period. The rationale is that an extended curing phase enhances the workability and durability of concrete. It was noted that the strength augmented with both the curing age and the proportion of eggshell substitution. The strength surpassed that of the control mix due to the incorporation of eggshell powder into the cement. Compared to the reference sample, the concrete made from eggshells shows superior early compressive strength during the initial curing phase. The interaction between silica in cement and calcium oxide from eggshell powder is augmented when cement is partly substituted with eggshell powder, owing to the persistent moisture from the process of cement hydration, which is a byproduct of the process. Additionally, filling the existing voids with eggshell powder makes the internal structure of the concrete more cohesive and leads to an increase in compressive strength. However, the additional increase in eggshell powder negatively affects the compressive strength at all curing ages.

3.3. Flexural Strength

The flexural strength results of the prepared composites are shown in Figure 11. As indicated in Figure 11a, the addition of CR to the composite mixtures led to an enhancement in their load-carrying capacity. Specifically, the included ECC mixture 25%, 50%, 75%, and 100% CR as replacements for sand exhibited increases in flexural strength of 2.6%, 11.3%, 26%, and 28.6%, respectively, this is in comparison to the control sample, which consists of sand as the fine aggregate. The maximum flexural strength, recorded at 7.4 Mpa, was observed for the mixture with 100% CR, while the minimum value, 5.75 Mpa, was noted for the control mixture CC. Introducing CR as a fine aggregate improves flexural strength due to its elastic properties and resistance to deformation through energy dissipation. This is what previous studies indicated about incorporating CR as an aggregate in traditional mortar and concrete [58].

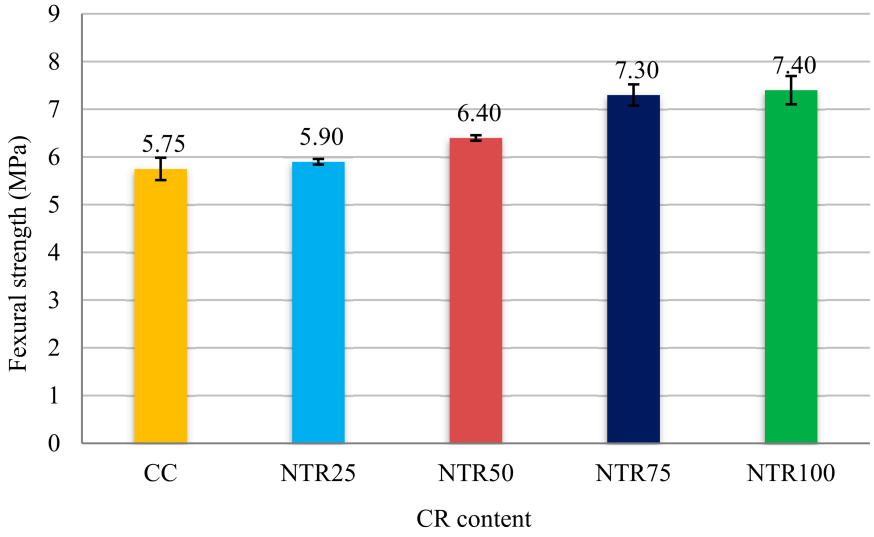

(**a**)

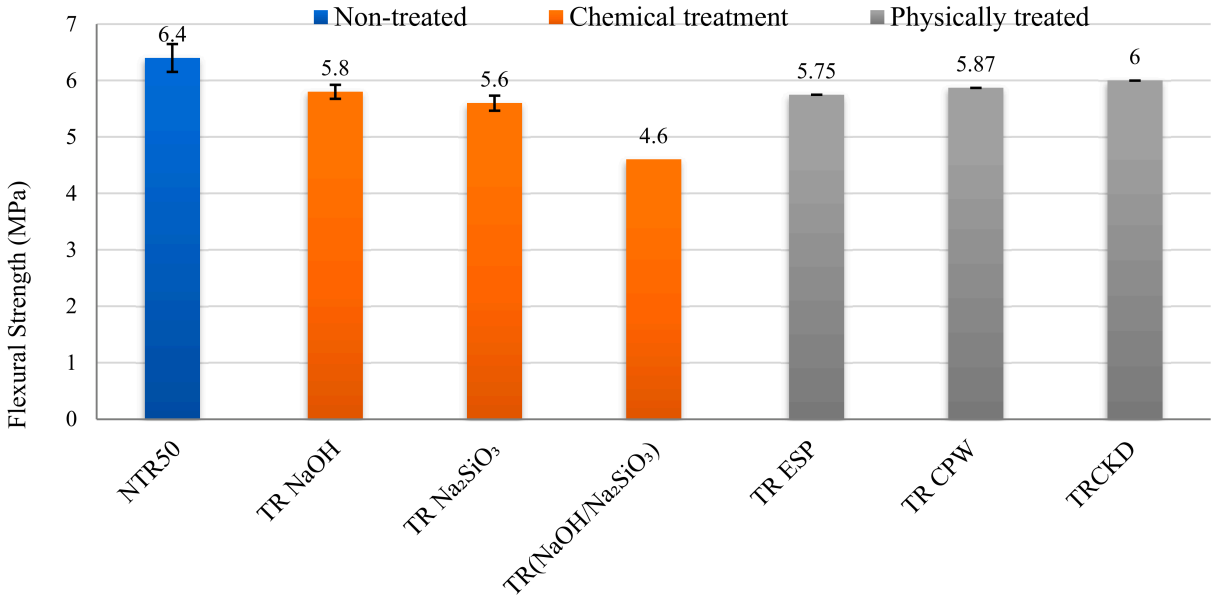

(**b**)

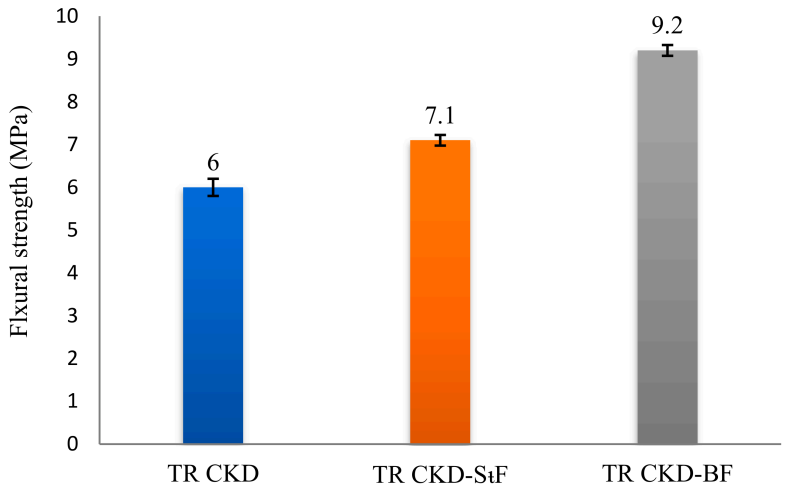

(**c**)

Figure 11. *Cont.*

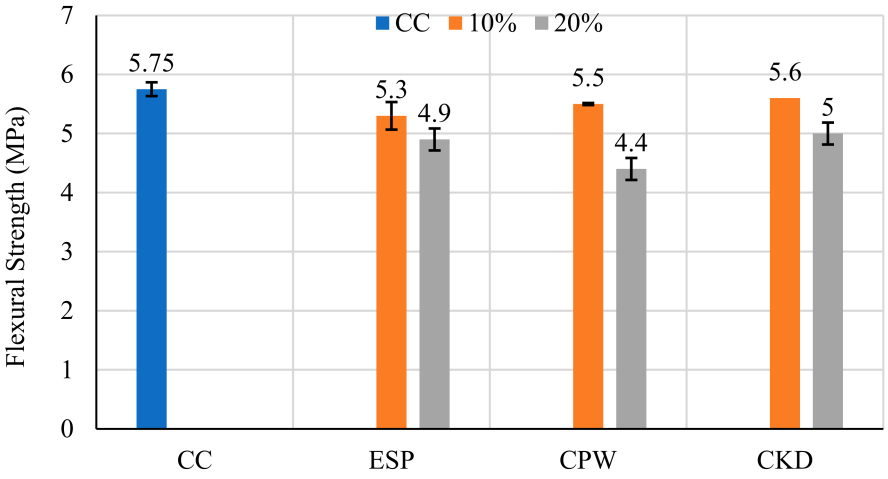

(**d**)

Figure 11. (**a**) Effect of CR content on ECC flexural strength. (**b**) Effect of chemical and physical treatments of CR on ECC flexural strength. (**c**) Effect of different types of fiber on EGC flexural strength. (**d**) The flexural strength of TR CKD and mix at 10 and 20% cement replacements.

Compared to physical therapy, the chemical treatment had less of an impact on flexural strength. The flexural strength of rubber concrete (CR-ECC) diminished from 6.4 MPa to 5.6 MPa when treated with sodium silicate, and further fell to 4.6 MPa with the combined treatment of sodium silicate and sodium hydroxide, resulting in loss percentages of 28.12% and 12.5%, respectively. The enhancements administered with NaOH markedly increase the bending strength of the rubberized concrete, exhibiting a 9% reduction relative to the reference sample (NTR50) as illustrated in Figure 11b.

The physical treatment of CR increased the bending strength of ECC (Figure 11b), although it remained lower than that of mixtures containing untreated CR. The observed improvement with untreated CR is attributed to the high elasticity of the rubber particles, which facilitates energy absorption and effective crack bridging under bending loads. Additionally, untreated CR improves flexural performance by increasing the ductility of the interfacial transition zone (ITZ) between the rubber and the cement matrix. In contrast, treated CR exhibits a stiffer coating and stronger bonding with the matrix, reducing particle deformability and limiting crack-bridging ability. Consequently, treatment decreases flexural strength despite enhancing compressive performance. These micromechanical interactions highlight the critical balance between particle elasticity, ITZ properties, and coating stiffness in controlling crack propagation and bending behavior of ECC mixtures containing CR.

Rubber is known for its high elasticity; however, treatment with NaOH or Na_2SiO_3 solutions slightly reduces elasticity. Nuzaimah et al. [65] reported a decrease in elongation at break for rubber treated with 1% NaOH compared to untreated rubber, although elongation slightly increases with higher NaOH concentrations, remaining below that of untreated CR.

The TR CKD, TR CPW, and TRESP combinations exhibited reductions in flexural strength of 6.3%, 8.28%, and 9.10%, respectively, when compared to the analogous mixtures prepared with untreated CR. The reduction in flexural strength associated with treated CR is ascribed to the coating produced by waste, which may modify the elastic properties of the rubber.

Upon comparison, with reference to Figure 11c, TRCKD-S_tF—which incorporates steel fibers—exhibited an 18% enhancement in flexural strength relative to TR CKD, which utilizes polypropylene fibers. The findings align with studies [66,67], indicating that while

PPF somewhat improves flexural strength, the incorporation of S_tF substantially increases it. PPF have a lower modulus of elasticity than S_tF fibers, so their tensile strength is lower, which affects the flexural strength of the samples. They are effective in filling fine cracks. On the contrary, steel fibers have a better modulus of elasticity and tensile strength, which significantly improves the flexural strength.

BF enhances the longevity of composite materials by vertically spanning cracks and striving to preserve the integrity of the composites, therefore mitigating the propagation of both big and minor fissures. Conversely, BF exhibits cracking at far smaller deformations than the control mix, although they markedly enhance the linear slope of the curve. The use of basalt fibers enhanced the flexural strength by 53.3% relative to the control sample.

It was observed that increasing the volume fraction of basalt fibers reduced the crack width in concrete, substituting larger cracks with finer ones. Previous studies have confirmed the effectiveness of basalt fibers in enhancing flexural performance [65], reporting that their addition can increase bending strength by up to 57%. Moreover, the inclusion of basalt fibers shifted the failure mode of concrete from brittle to ductile, in agreement with findings from other relevant investigations [68].

As shown in Figure 11d, the flexural strength value started to decrease after the ESW was added into ECC. The flexural strength started decreasing compared to the control mix that contains 50% CR treated with CKD (TRCKD). The highest flexural strength recorded was 5.3 MPa on the 28th day of curing. At a 20% content, the lowest recorded bending strength is 4.9 MPa, while 10% gave a higher value, but it remains lower than the reference mix strength.

The free lime present in CKD is less than 10%, and therefore it does not possess high cementitious properties [58]. The strength decreases when replacing cement with CKD due to the reduced cement content. This is accompanied by a decrease in flexural strength relative to the reference mix, which exhibits the maximum flexural strength. The substitution of 10% does not have a detrimental effect on flexural strength. At replacement rates of 10% and 20% of Portland cement with CKD, the reduction in flexural strength values after 28 days was 4.3% and 23%, respectively.

The flexural strength of the control mix is 5.75 MPa. The flexural strength of concrete containing 10% and 20% CPW is 5.5 and 4.4 MPa, respectively. On the contrary, the flexural strength of ECC containing CKD, CPW, and ESW as partial cement replacements was enhanced. Compared to the control mixture CC, Figure 11d shows an improvement in flexural strength when using CKD, CPW, or ESW by 16.2%, 12.6%, and 14.6%, respectively, at a 10% replacement rate, and by 24.1%, 21.5%, and 23.0%, respectively, at a 20% replacement rate.

The results cited above suggest that an ideal replacement ratio of 10% produces the best outcomes. This can be attributed to the pozzolanic activity of ceramic powder employed, which are primarily composed of SiO_2, CaO, and Al_2O_3. These components enhance the formation of high-quality calcium silicate hydrate (CSH), thereby improving the ITZ. Additionally, the incorporation of ESW and CKD as fine fillers further contributes to the improved concrete matrix. Nevertheless, the observed reduction in flexural strength with the utilization of treated rubber (TCR) appears to result from the coating formed on the CR by the waste materials, which may alter the elastic properties of the rubber particles. A major observation from 11d is that, in general, it shows a reduction in flexural strength with an increase in the substitution ratio of ESW, CPW, and CKD.

3.4. Uniaxial Tensile Strength

The standard tensile load–displacement curves for the ECC mixtures assessed after 28 days are presented in Figure 12. Looking at the pictures, there are three separate regions on the displacement curve for the tensile load. The first stage (pre-cracking) ends with the

appearance of the first crack at the beginning of loading. The second (post-crack) occurs between the initial crack and the maximum load. The third (failure zone) begins after the ultimate load and continues until the sample fails. All ECC mixes showed clear strain hardening properties.

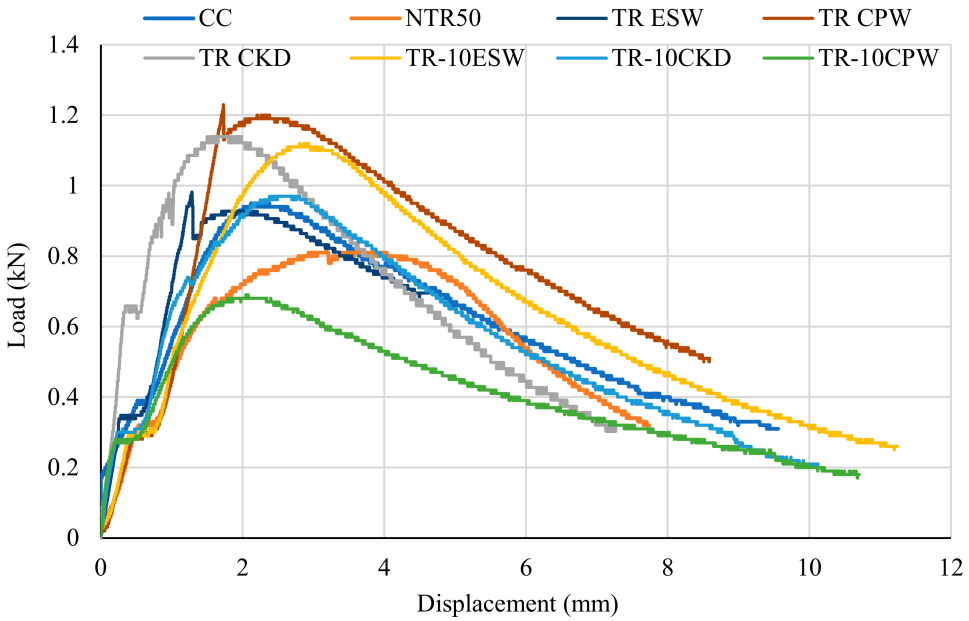

Figure 12. Load–displacement curves of ECC uniaxial tensile strength test.

The uniaxial tensile strength results indicate that the mixtures using cement kiln dust for CR treatment achieved the highest maximum loads among all the tested mixtures. The control specimen exhibited a maximum tensile strength of 0.98 MPa at 28 days. In comparison, specimens incorporating untreated crumb rubber demonstrated reductions in split tensile strength by 14.4%, 16%, 20%, and 26% relative to the control mix at rubber contents of 25%, 50%, 75%, and 100%, respectively. This decrease in strength is attributed to mechanisms similar to those causing the decline in compressive strength. Notably, specimens containing treated rubber showed enhanced tensile strength.

The obtained result revealed that the incorporation of the NTR50 mix resulted in a decline in tensile strength of 18.2% compared to the control CC mixture. This reduction in strength is due to inadequate cement paste coating on the non-treated CR area and poor particle gradation in the NTR50 mixture. Whereas, the findings of the mixtures with 50% of the CR treated physically showed a greater uniaxial tensile strength of 16.4% and 14.2%, respectively using CKD and CPW, compared to the traditional CC mix, shown in Figure 12. The pozzolanic behavior, as well as the coarse texture and irregular shape of the physically treated CR elements, contributed to the increase in tensile strength. This process enhanced the bond between the cement paste and the particles of the cured materials [36]. While CKD acted as a filler, it filled the existing pores due to the precision of its particle size, which enhanced the internal structure density of the concrete and increased its tensile strength.

According to Figure 12, the tensile strength commenced an increase at a 10% replacement of eggshell powder relative to the control mix. When eggshell powder is added, the tensile strength increases, reaching a maximum value of 26.6 Mpa at 28 days of curing. It was noted that the tensile strength rises with the percentage of ESW at 10%, after which the strength begins to decline [59]. Partially replacing cement with ESW enhances the reaction between the calcium oxide in ESW and the silica present in cement, which is a result of the cement hydration process in the absence of continuous moisture. Moreover, the existing pores are filled with ESW, where it acts as an additional filler, filling the existing pores, thus enhancing the density

of the concrete's interior structure and resulting in increased tensile strength. Nonetheless, an additional increase in ESP will decrease compressive strength in all treatment ages.

Among all tested groups, the specimen designated TRCKD achieved the highest tensile strength, outperforming both treated and untreated counterparts. When 10% of the cement was substituted with ceramic powder in conjunction with 50% treated rubber (TRCPW), a reduction of 20% in tensile strength was observed. On the other hand, tensile strength increased by 15% in comparison to the control mix when 10% of the cement was substituted with cement kiln dust and 50% treated rubber.

This data indicates enhanced the effectiveness of these particular mixtures emphasizes that the approach of substituting 50% of the sand with physically treated CR and 10% of the cement by CKD, is especially efficacious. Thus, this method not only raised the highest load capacity of ECC, it also markedly improved its general structural performance. The results suggest that a 10% cement substitution may be an effective method for enhancing the strength of ECC materials in practical applications.

3.5. Sorptivity

The surface quality of concrete can be identified through the capillary property index. It also provides information on the continuity of capillaries and the structure and size of pores, which determine the water absorption capacity of concrete and its transfer in an unsaturated state [69].

To prepare the absorption test samples, three disks were taken from the middle part of the cylinder with a diameter of 100 mm and a thickness of 50 mm to ensure the uniformity of the samples in quality and reduce the variation between them. A summary of absorption values and coefficients for ECC mixtures is shown in Table 4. Figure 13 illustrates the connection between the square root of time and the average cumulative water absorption per unit area. As seen in Figure 13a,b, the peak water absorption occurs at the beginning of the test before it starts to gradually decline.

Table 4. Water absorption values and sorptivity coefficients of all ECC mixes.

NU.	Groups	Mix Code	Si ($\times 10^{-3}$ mm/s$^{0.5}$)	Ss ($\times 10^{-3}$ mm/s$^{0.5}$)	ΔWi (g)	ΔWs (g)	ΔWt (g)
1	Control mix ECC	CC	13.2	3.2	12.7	8.3	21.0
2	Non-treated CR replaced sand	NTR25	13.9	2.9	15.1	6.6	21.7
3		NTR50	11.5	3.1	10.0	8.0	18.0
4		NTR75	14.3	4.4	11.7	11.7	23.4
5		NTR100	15.6	4.8	12.7	12.3	25.0
6	CR treated using NaOH	TR NaOH	12.1	2.4	11.9	3.7	15.6
7	CR treated using Na_2SiO_3	TR Na_2SiO_3	7.9	3.2	7.3	11.1	18.4
8	CR treated using NaOH/Na_2SiO_3	TR NaOH/Na_2SiO_3	13.8	4.4	12.4	9.3	21.7
9	CR treated using ESW	TR ESW	13.4	3.0	12.2	5.4	17.6
10	CR treated using CPW	TR CPW	11.8	3.1	9.4	7.0	16.4
11	CR treated using CKD	TR CKD	9.3	2.8	7.8	6.6	14.4
12	CR treated using CKD, with BF	TR CKD-BF	8.2	2.2	9.4	4.3	13.7
13	CR treated using CKD, with S_tF	TR CKD-S_tF	4.7	1.7	4.8	6.1	10.9
14	CR treated using CKD, with ESW replaced cement	TR-10 ESW	4.7	2.0	4.4	7.4	11.8
15		TR-20 ESW	7.4	4.6	6.8	17.2	24.0
16	CR treated using CKD, with CDK replaced cement	TR-10 CDK	6.1	3.0	5.8	10.5	16.3
17		TR-20 CDK	4.8	2.1	4.2	7.8	12.0
18	CR treated using CKD, with CPW replaced cement	TR-10 CPW	5.0	2.2	4.7	7.8	12.5
19		TR-20 CPW	13.5	4.6	12.4	13.5	25.9

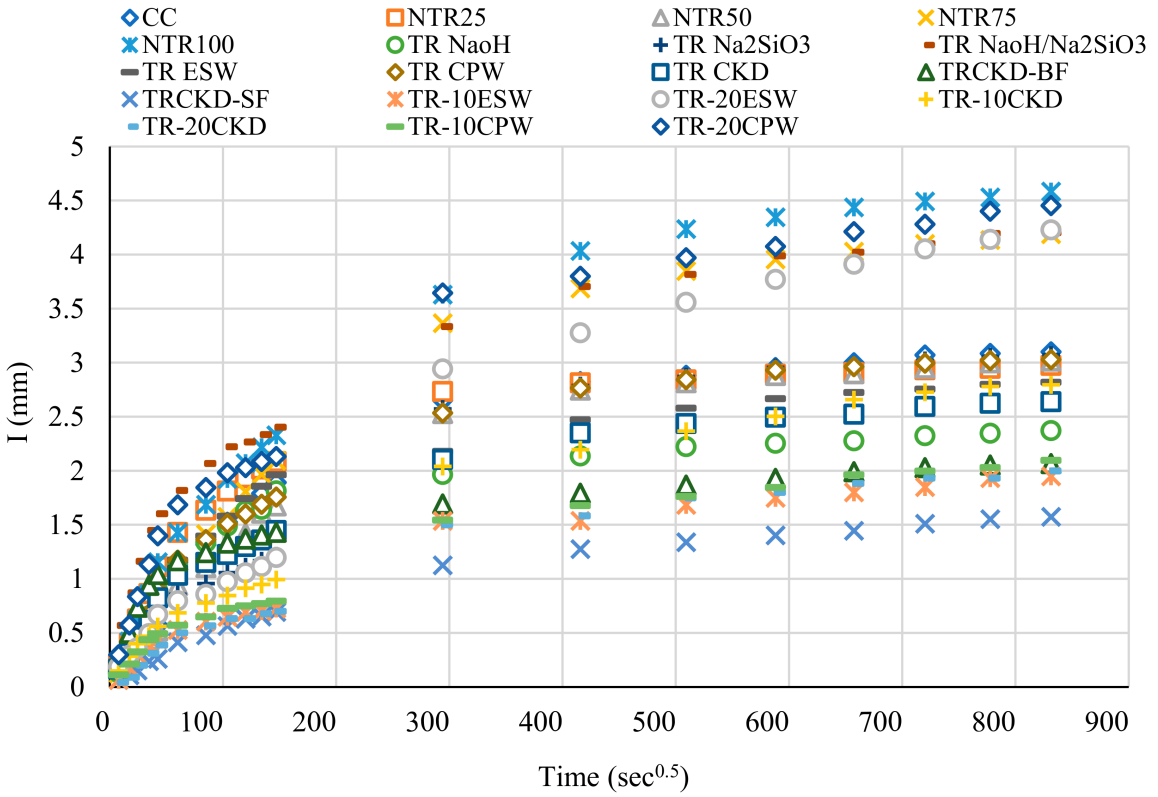

(**a**) Overall water absorption over 8 days.

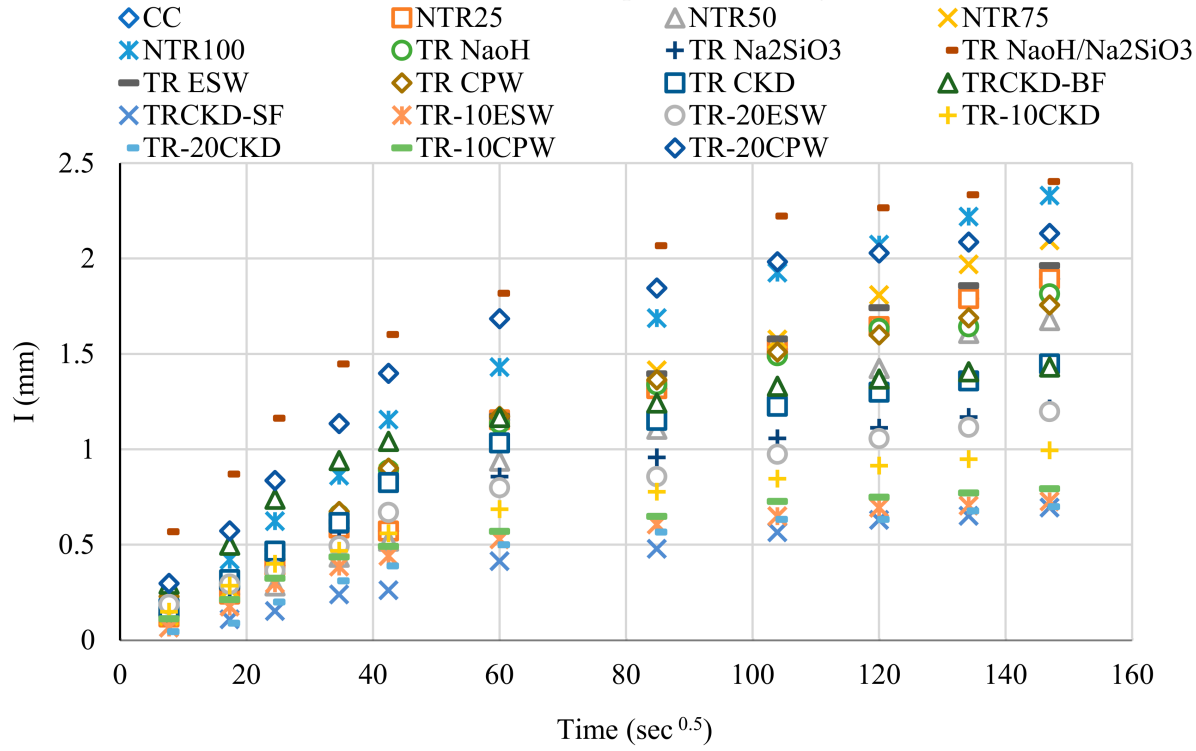

(**b**) Zoomed-in view of the initial 6 h of capillary absorption.

Figure 13. The capillary absorption changed over time for all ECC mixtures on the 28th day.

From the results, it is clear that ECC mixtures containing unprocessed rubber have the highest absorption coefficient values. Due to the internal pores resulting from the presence of unprocessed rubber in the ECC mixture, there was an increase in the absorption rate. Accordingly, proportional reduction ratios for the mixtures are observed in harmony with

the rubber content in the mixtures as follows: 25%, 50%, 75%, and 100% of untreated CR to 3%, 20.5%, 30%, and 38.3%, respectively, compared to the control CC mix. Due to the presence of rubber in ECC, there are many inaccessible pores within the cement paste, which increases the high air content. And consequently, it has a high air content. The weak bond between CR and the matrix creates more accessible pores for water penetration, which in turn reduces the impact of the paste's porosity.

In contrast, the physical treatment of CR and its incorporation at 50% into ECC reduced water absorption per unit area and enhanced all absorption parameters; see Figure 13 and Table 4. Furthermore, treating 50% of CR using ESW, CPW, CKD, and replacing sand contributed to reducing the water absorption rate 1.2%, 11.11%, and 20%, respectively, Compared to the NTR50 sample mixture. The decrease in the water absorption property of ESW particles and the filling provided by CPW and CKD in the NTR50 matrix is what generally improved the absorption of the samples. Additionally, high water absorption properties in CKD and CPW particles also effectively contribute to this property.

In the identical direction, the water absorption capacity per unit area and all absorption standards of the ECC mixtures containing ESW, CPW and CKD as a 10% cement substitute improved. These mixtures showed a decrease in water absorption values and standards by approximately 8.3%, 12.5%, and 34%, respectively, compared to the reference NTR50 mixture. Combining waste with ECC effectively reduces its water absorption according to the results. The introduction of waste materials used in appropriate quantities as a substitute for cement ideally reduces water absorption due to the improved secondary hydration reactions of the waste, resulting in the formation of C–S–H, which reduces capillarity due to the densification of the microstructure of the ECC mix. Moreover, partially replacing cement with waste materials is one way to improve the water resistance of engineered cementitious composites (ECC). The reduction in cement content results in a decrease in hydration products, and consequently, the water absorption capacity increases at a waste ratio of 20%, which cannot fill the pores in ECC.

Among the mixtures containing chemically treated rubber, the CR treatment using Na_2SiO_3/NaOH mixture showed the highest absorption rates, with water absorption values and standards of approximately 21.1%. Meanwhile, the CR treatment using NaOH mixture showed a decrease in water absorption values by 3.2% compared to NTR50 mixtures.

As presented in Table 4, both the initial and secondary absorption values were evaluated for the prepared mixtures. Notably, the mixtures incorporating CKD and 50% rubber as a sand replacement, along with S_tF, demonstrated reduced absorption rates of 2.1 and 1.1, respectively. These values are lower than those observed in all other treated mixtures containing the same proportion of rubber crumb. This indicates that the combined use of cement kiln dust and S_tF contributes to a significant decrease in water absorption in high-rubber-content mixtures.

Steel fibers used with NTR50 mixtures showed a decrease in the amount of water absorbed per unit area compared to basalt and polypropylene fibers. Where S_tF acts as a barrier to water flow, it limits water leakage. Additionally, the steel fibers can reduce the fine cracks resulting from the heat of hydration reactions [61]. Compared to PPF, basalt fibers showed a decrease in water absorption at the same mix ratios, with better dispersion and less agglomeration of basalt fibers behind this improvement. Which gives it greater effectiveness in enhancing durability due to its reduction in capillary pores.

The reduction percentage for the mixture containing S_tF and BF in equal proportions was 2% of the mixture volume. These mixtures showed a decrease in water absorption values and standards by nearly 23% and 5.6%, respectively, compared to the TRCKD mixture which used polypropylene fibers.

3.6. Acid Attack—Strength Changes

Figure 14 shows the decrease in compression strength following immersion periods of 28, 58, 120, and 180 days in a 4% H_2SO_4 solution. The compressive strength of CC decreased by 11.76% and 13% at 120 and 180 days, respectively, this indicates the deterioration of the fine internal structure in the control mix due to corrosion from acid infiltration, putting the structural integrity at risk.

Concrete specimens cured in water and those submerged in a 4% Na_2SO_4 solution were compared for compressive strength, as shown in Figure 14a. This comparison encompasses both control CC and ECC mixes in which CR was used as a partial substitute for sand and was evaluated under both water curing and sodium sulphate immersion (Na_2SO_4) conditions. Across all mixes, specimens subjected to water curing irrespective of rubber incorporation demonstrated a consistent increase in compressive strength with prolonged curing periods. Furthermore, Figure 14a displays the reduction in compressive strength observed after exposure to a 4% H_2SO_4 solution for 56, 120, and 180 days. Specifically, the CC sample exhibited compressive strength losses of 10.2%, 7.3%, and 8% at 56, 120, and 182 days, respectively. These results suggest that immersion in sulfuric acid significantly undermines structural integrity, primarily due to acid-induced leaching and the subsequent deterioration of the concrete's internal microstructure in control mixture.

The compressive strength decreased by 12.28%, 4.4%, and 8% for the NTR50 model at 56, 120, and 180 days, respectively. These results are consistent with those reached by [62,64], which indicate a direct relationship between the increase in CR content, the appearance of micro-cracks, and the increase in porosity, causing weight loss and strength deterioration under acidic conditions.

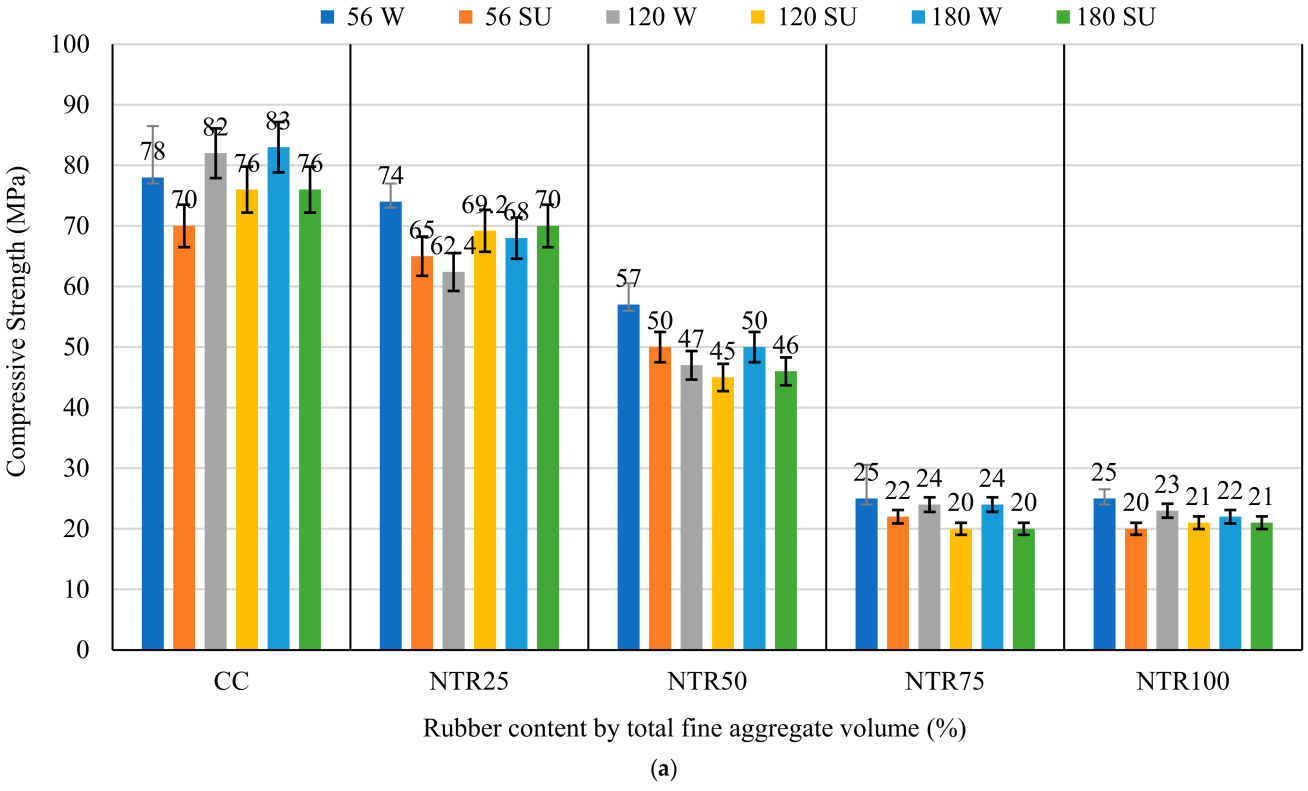

Figure 14. *Cont.*

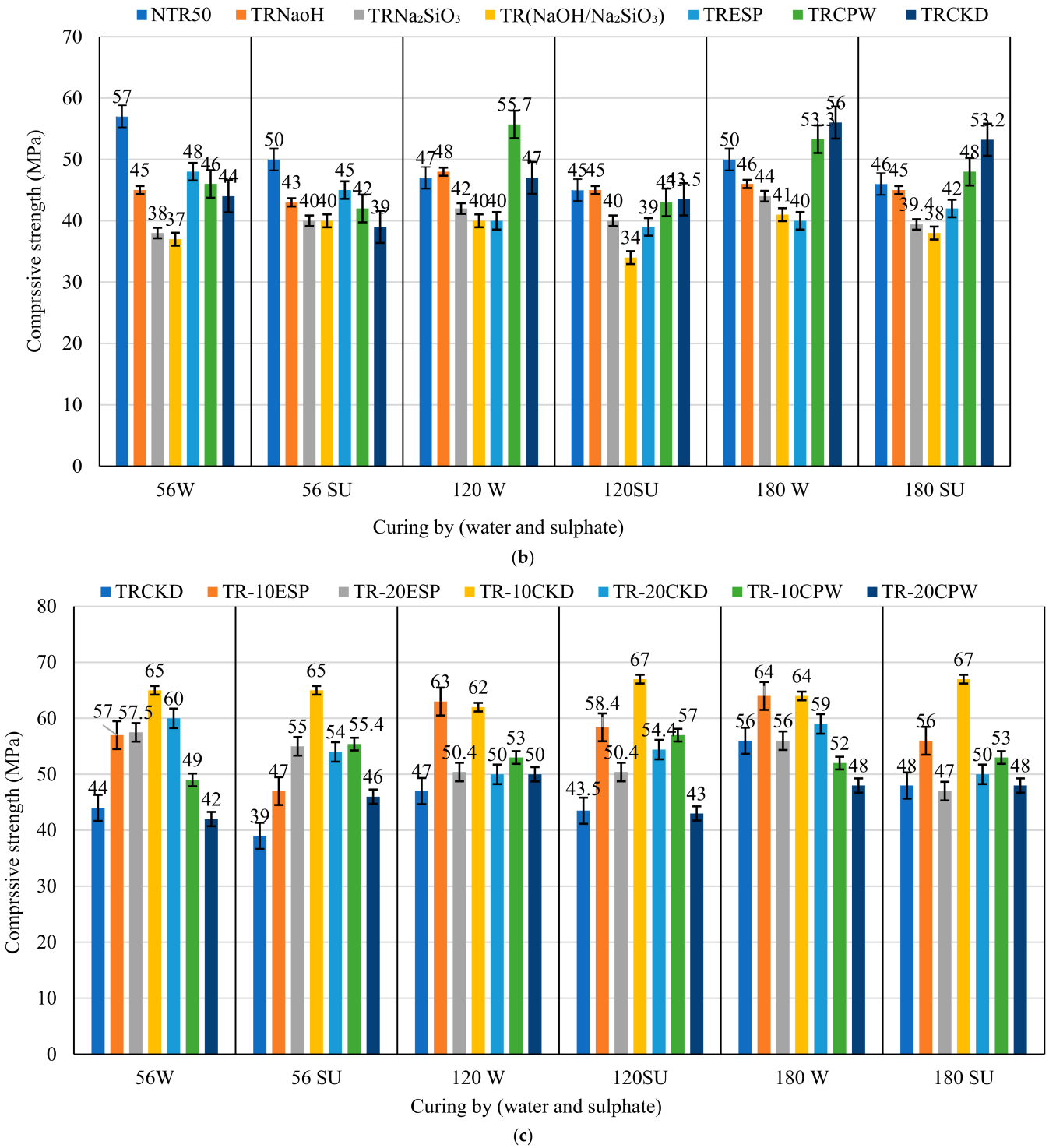

Figure 14. (**a**) Compressive strength comparison of CR-ECC: Cured in water (W) and immersed in 4% sodium sulfate (SU). (**b**) Compressive strength comparison of treatment TR-ECC: Cured in water (W) and immersed in 4% sodium sulfate (SU). (**c**) Compressive strength comparison of TR CKD and replacement cement (10, 20%): Cured in water (W) and immersed in 4% sodium sulfate (SU).

When the NTR25 samples were assessed and submerged in sodium sulfate, it was found that there was an initial increase in strength that strength improved initially, followed by a decrease at the end of the immersion period, at 180 days. However, at the end of the soaking period in the sodium sulfate solution, it was found that the strength was equal to its original strength. The material's enhanced strength is ascribed to the higher formation of C–S–H gel as a secondary product, along with expansive products arising from reactions

between hydration products and sodium sulfate solution during immersion. The formation of extension products led to cracking and flaking, resulting in reduced strength. The highest reduction value in compressive strength was found for the reference mix with 25% rubber at 56 days, and the lowest reduction value was found for the same mixture at 120 and 180 days exposed to 4% Na_2SO_4.

It was found that at a 50% replacement ratio of physically treated rubber crumbs, an improvement in sulfate resistance was observed compared to chemically treated ones, Figure 14c, and it was noted that this resistance decreases as the amount of rubber in the concrete increases. Because the treated rubber particles in the rubberized concrete prevented fracture development and physical disintegration, the untreated control mix samples showed the greatest loss in durability.

The treatment of CR with cement kiln dust and ceramic powder plays important roles in improving the durability of ECC, as an increase in sulfate resistance of 1.15 and 1.04 was observed, respectively, in harsh environments. Therefore, it is obvious that the TR-ECC processor is successfully resistant to the harmful environment Figure 14b. The findings of the test can be explained by observing modifications in the values of the two existing parameters, which are NTR and TCR. The CR particles existing in the CR-ECC caused microcracking cracks in the specimens, allowing the acidic medium to penetrate more deeply. However, in TR-ECC with CKD or CPW, fewer cracks grew, and the constituent materials had separated less.

Concrete exposed to Na_2SO_4 solution with a replacement ratio of 10% and 20% for cement (using CDK, CWP, and ESW) showed improvements in compressive strength over the exposure period, indicating that exposure to the solution does not negatively affect the mechanical strength of these mixes.

All samples with a 10% replacement ratio exhibited a slight increase in average compressive strength compared to their counterparts cured in water, as shown in Figure 14c. In contrast, when the replacement ratio was raised to 20%, the mixes experienced a reduction in strength after 120 and 180 days of exposure (refer to Figure 14c). Specifically, the TR-20ESW, TR-20CKD, and TR-20CPW mixes recorded strength losses of 16%, 15%, and 1%, respectively, relative to the water-cured specimens. After 180 days, the reference mix TR CKD showed a 14% decrease. The results of this study suggest that there are two distinct stages in the formation of compressive strength.

At early curing ages, an increase in compressive strength was observed for all mixtures except those in which cement was partially replaced with eggshell powder. This enhancement is attributed to the predominance of hydration reactions during the initial stages, leading to the formation of ettringite. The generated ettringite occupies the pore spaces within the concrete matrix, contributing to an overall improvement in strength [70]. However, at later curing ages, deleterious chemical reactions become more pronounced, adversely affecting the mechanical performance of the mixes. The observed decrease in strength is primarily associated with the presence of gypsum and the formation of secondary ettringite. These expansive phases contribute to microstructural deterioration and subsequent strength loss. This transition in behavior underscores the impact of processing time on the durability and performance of the materials under study.

The average loss in compressive strength at the 180th day for the reference TRCKD, TR-10ESW, TR-10CKD, and TR-10CPW mixes subjected to Na_2SO_4, compared to their water-cured equivalents, was 1.4%, −16%, −4.7% and 12%, respectively, as illustrated in Figure 14c.

4. Microstructure

The microstructure and morphology of cement paste, as well as the interfacial transition zone between small particles and paste, were examined in this work using SEM examination. Additionally, the distribution of Mg, Ca, Si, and Fe elements was ascertained and the composition of the selected ECC mixtures was carefully examined using EDX analysis.

The cement pastes SEM images for the following ECC mixes CC, NTR50, TR CKD, TRCKD-BF, TR CKD-S_tF, and TR-10CKD at 28 days reveal substantial microstructural variations based on the used materials. In the control mix CC illustrated in Figure 15a, the SEM images reveal a dense and homogenous matrix with uniformly distributed particles, resulting in a robust and durable cement paste. This compact microstructure improves the mix's general durability and strength, signifying low porosity and superior bonding within the matrix. These features point to well-hydrated cement pastes with optimal particle and hydration product distribution, like C–S–H, which enhances the mechanical performance of the mixture.

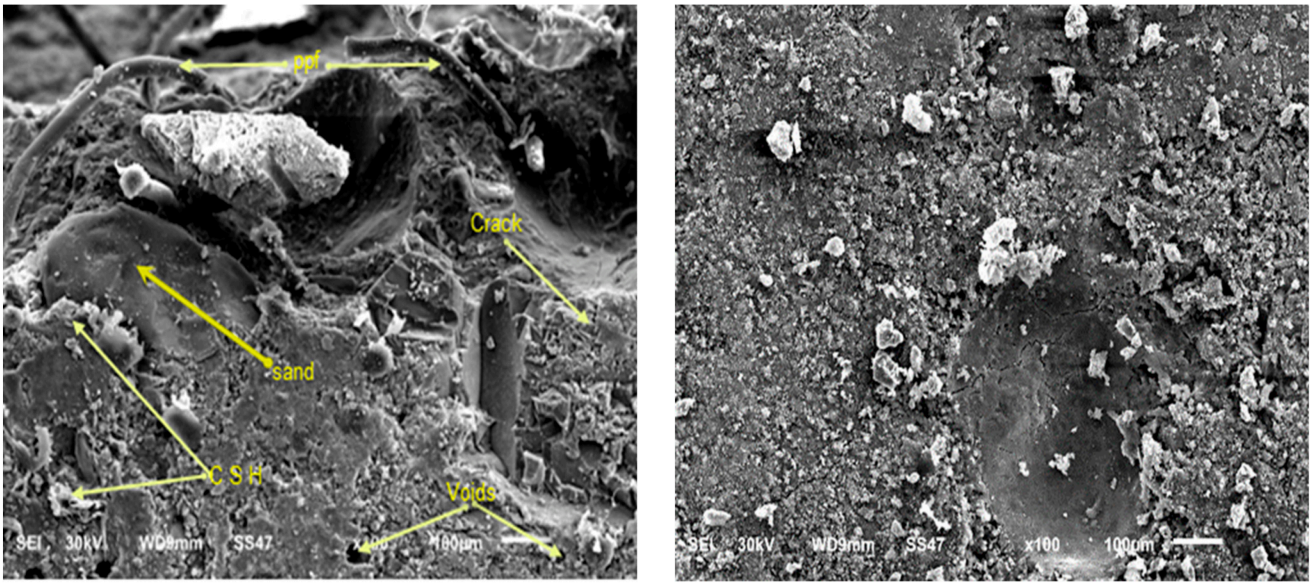

(**a**)

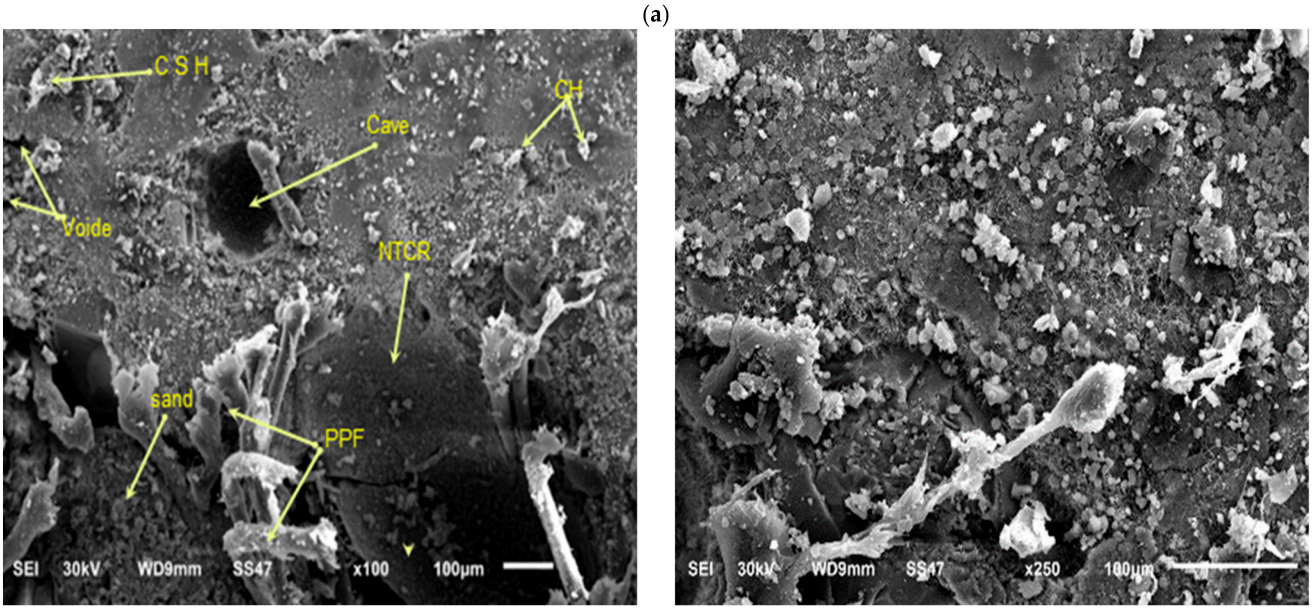

(**b**)

Figure 15. *Cont.*

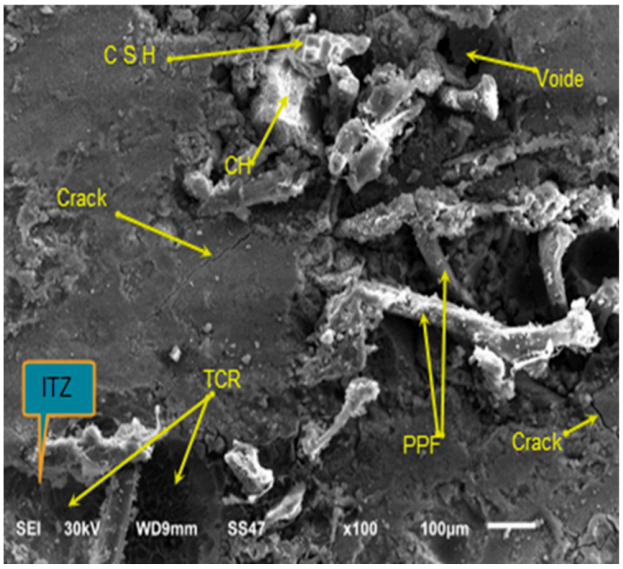

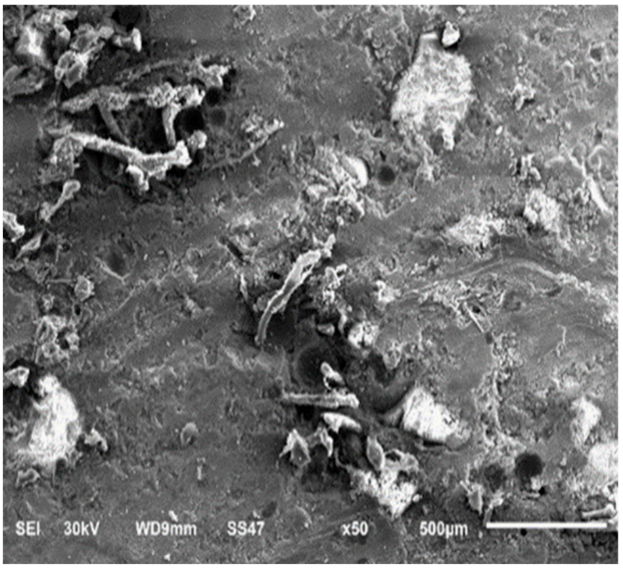

(**c**)

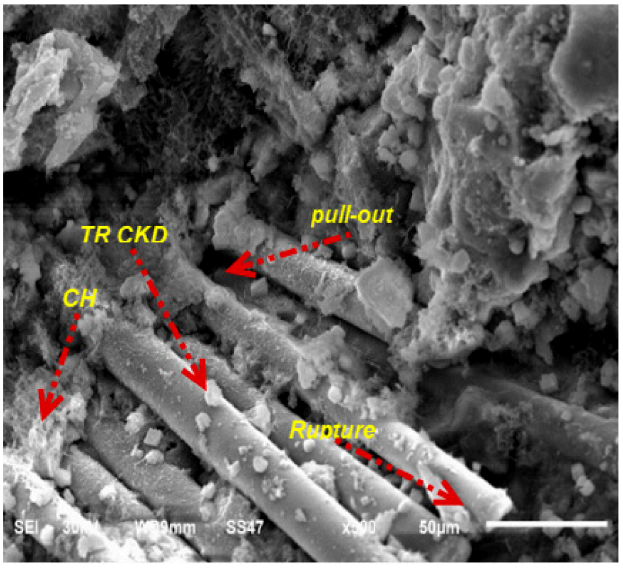

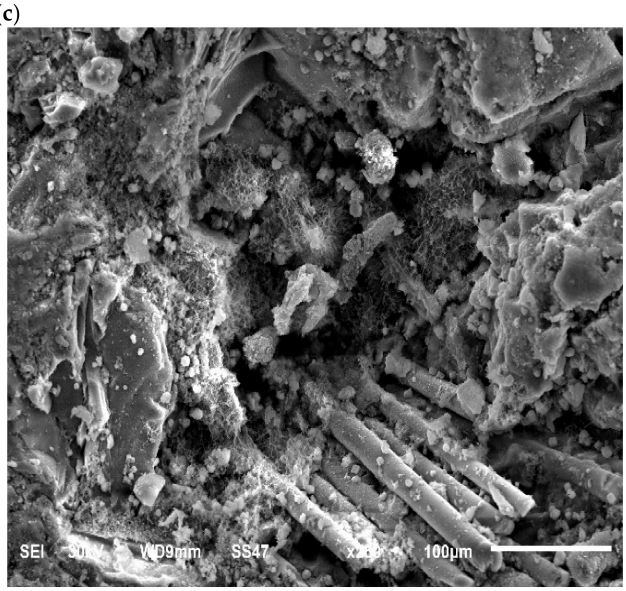

(**d**)

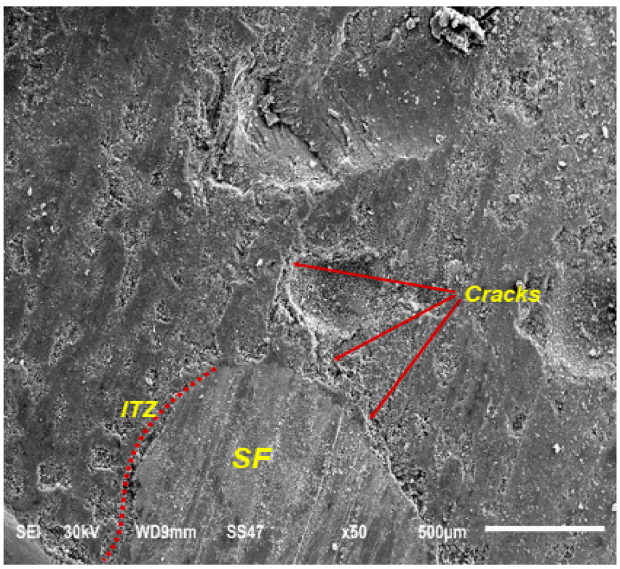

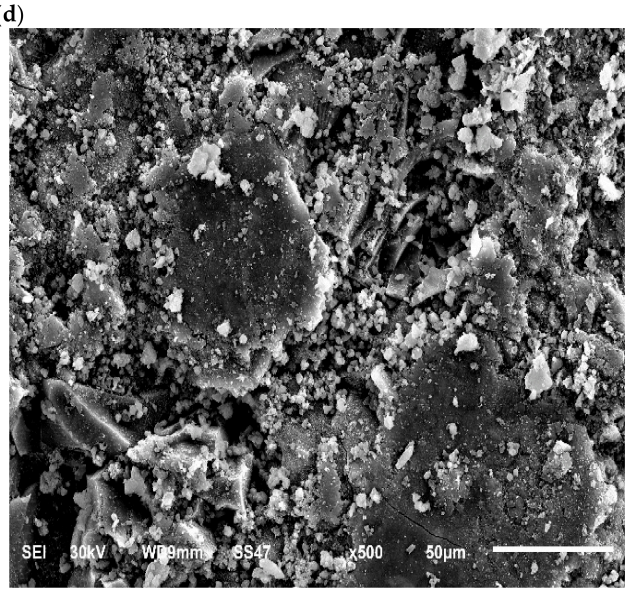

(**e**)

Figure 15. *Cont.*

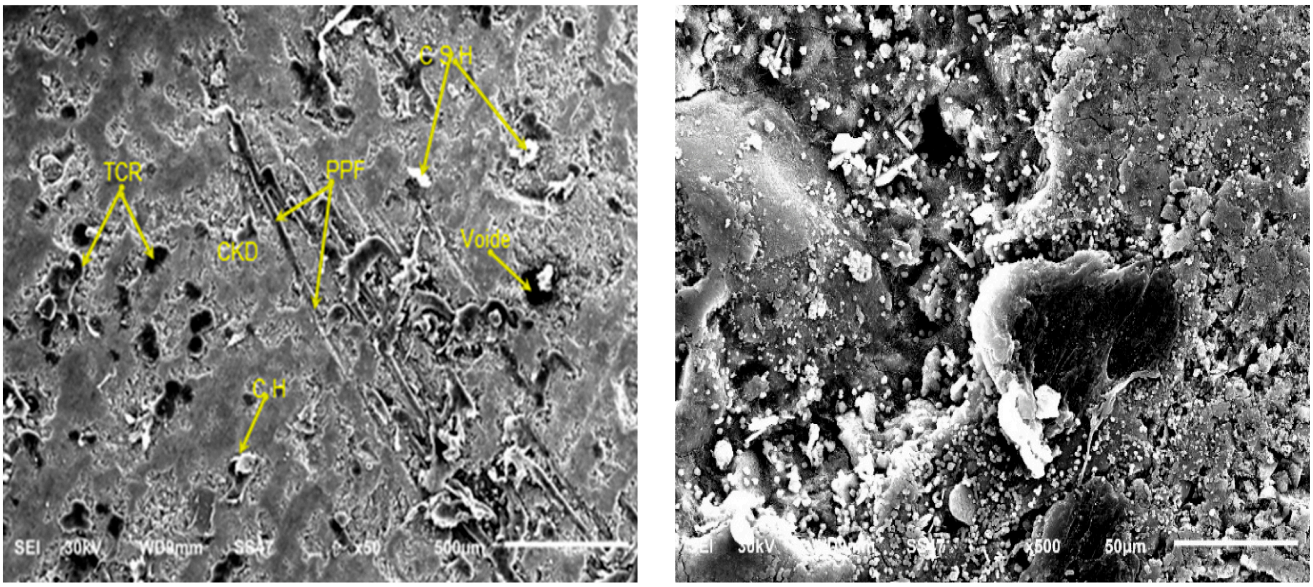

(**f**)

Figure 15. (**a**) SEM images of CC mix. (**b**) SEM images of NTR50 mix. (**c**) SEM images of TR CKD mix. (**d**) SEM images of TRCKD-BF mix. (**e**) SEM images of TRCKD-S_tF mix. (**f**) SEM images of TR-10CKD mix.

4.1. Morphology of NTR50

Figure 15b is the SEM of NTR50 particles at a magnification of 100×. Two nearby molecules with entirely different textures were selected at random. The particle surfaces are shown in the picture, with a rough and porous surface on the right and a smooth and angular surface on the left. The particle on the right side originated from the top layer of the frame, but the particle on the left may have been taken from the inner layer. Due to the very smooth surface of the particle on the right side, less bonding between the cement pastes and CR is expected. Moreover, the presence of small cavities has been observed. The particle's left-hand surface, in contrast, shows several small cavities that are difficult for the cement paste to penetrate, in addition to one large cavity. Therefore, the bond between CR and the cement paste is weaker.

Figure 15 shows many solid materials adhering to the surface of the rubber crumbs, which is often the case—in addition to oils, dust, and other impurities [71]. This adds to the tenuous connection between the cement mortar and CR particles. Bisht and Ramana [72] explained that the shape and surface texture are responsible for the weak bonding between the cement mortar and CR. Therefore, to ensure better adhesion, the rubber should be treated to obtain a suitable rough surface and remove any adhering impurities.

4.2. Morphology of TR CKD

Figure 15c shows the SEM of the CKD-treated CR particle. After applying the CKD coating, we observed a significant change in the morphology compared to the untreated CR particles. The CKD paste improved the workability and particle distribution during the mixing and pouring of TR CKD due to its penetration into the cavities and filling of them; it also reduced the angularity on the CR surface. Moreover, the CKD coating technique overcame the hydrophobic nature of CR. Therefore, it significantly reduces the trapped air associated with the introduction of CR, thereby enhancing the bond between TR CKD and ECC mortar. Nevertheless, we found some microcracks and a few gaps in the cement kiln dust coating, which we expect to be easily addressed during the concrete mixing.

4.3. Morphology of TRCKD-BF

Figure 15d illustrates the contribution of basalt to enhancing the cement matrix, energy consumption can be observed due to the occurrence of pulling, fracturing, calcification, severe friction, and slipping [67]. The basalt fibers have a favorable relative distribution that can also be observed. Usually, the fibers that fray away from the crack plane are the ones that enhance the fiber bonding process through the reinforcement pulled from them. The composite gains its strength by dissipating the compressive frictional energy that supports advancing cracks when the fibers are pulled from the matrix. SEM micrographs show the responsibility of this mechanism for the observed hardening in composite materials containing fibers [73,74]. Figure 15d of the SEM illustrates the results of the uneven and poor distribution of basalt fibers. The bending of the fibers and the agglomeration cause a decrease in strength: pullout, rupture, fossils of basalt fibers, and also calcium hydroxide (CH) crystals.

4.4. Morphology of TRCKD-S_tF

In Figure 15e, SEM images show ECC mixtures with 2% steel fiber S_tF. It decreased the voids in the transition zone between the cement mortar and the short fibers and strengthened the connection. Because the cementitious matrix is thickly covering the steel fibers' surface, the images show a strong bond between the fibers and the cement. Due to the hardening and shrinkage of the cement paste, fine cracks are observed in the ITZ area in TRCKD-S_tF [75,76]. Micro-cracks initially form in the weak areas of the interface due to the increased internal pressure within the ITZ region, which causes defective microcracks. As shown in Figure 15e, when faced with S_tF, their directions change.

4.5. Morphology of TR-10CKD

Figure 15f shows that the TR-10CKD mix, which has 10% of its cement replaced with CKD, exhibits the density and uniformity of the microstructure of the sample. CKD particles serve as nuclei for hydration products, contributing to the formation of C–S–H. The reduction in porosity and the good distribution of particles in the matrix densification enhance both compressive strength and durability. In addition to the fact that using CKD is environmentally friendly, SEM images of TR-10CKD show its benefits as a successful partial substitute for cement, as it has maintained the strength and integrity of the matrix. Through this analysis, the importance of selecting and processing materials in the microstructural properties of ECC can be identified. Mixtures such as 10% CKD and 20% CKD showed clear, substantial enhancements in the microstructural integrity and overall performance.

An SEM test was carried out on samples containing treated and untreated rubber crumb to determine the morphology of CR. Using SEM, the following structure can be identified: surface, crystalline, and chemical composition, in addition to electrical behavior. The study also examined the crystal structure and electrical behavior of the tops [77]. Since surface treatment of rubber was the basis of this research, SEM technology facilitated the examination of the physical effects of surface treatments in addition to the experimental results of the chemical effects of surface treatments. From Figure 15a–e, it appears that the surface treatment of CR with CKD made it rougher than the other five methods, as evidenced by the pressure test. After CKD, surface treatment with TR CPW ceramic powder was the best compared to samples treated with NaOH and detergents, resulting in the second-best outcomes. The CR surfaces coated with CPW, ESW, and $NaOH/Na_2SiO_3$ had a slightly rougher texture than the untreated CR surfaces.

5. EDX Analysis

As indicated in Figure 16, the comparative analysis of EDX patterns reveals the different additives embedded in the cement matrix and their elemental composition for four ECC mixtures (CC, NTR50, TRCKD, TRCKD-BF, TRCKD-S_tF, and TR-10CKD). The control mixture (CC) had the appearance of a typical cementitious compound, with a high content of oxygen and calcium, The high content of silicon and aluminum elements in both SF and GGBFS is involved in the manufacturing of cement hydration products such as C–S–H and CH. It enhances the density and strength of the matrix. The robust and durable characteristics of the control mix is attributed to the excellent and balanced distribution of the elements, making it a benchmark for comparison with the compacted mixtures (Figure 16a). On the contrary, the high calcium content in the TR CKD mixture reflects the significant input of untreated CR, which was partially replaced with cementitious components (Figure 16b).

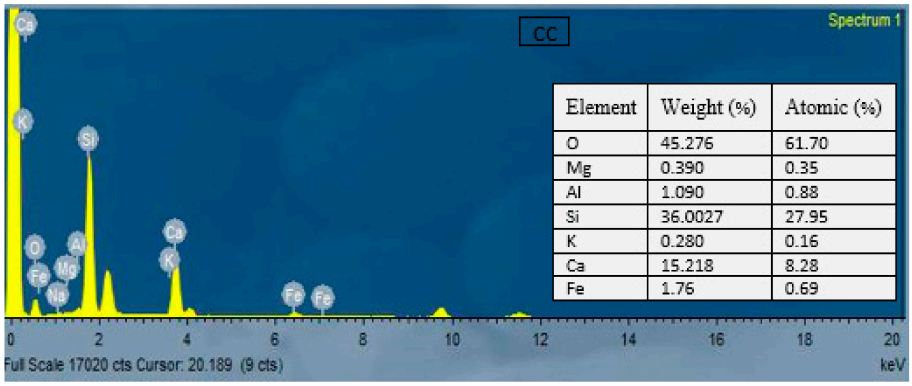

(**a**)

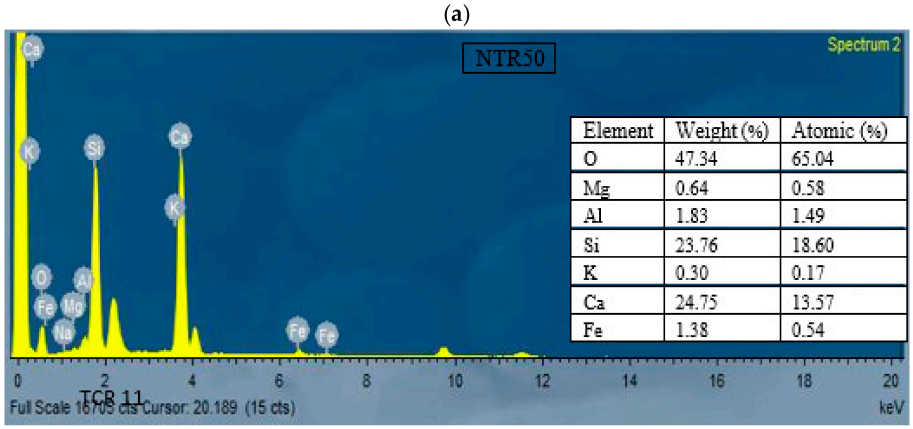

(**b**)

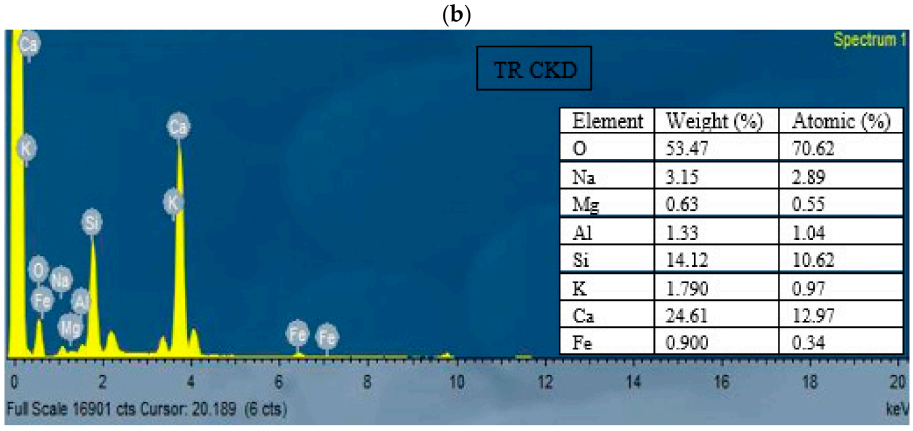

(**c**)

Figure 16. *Cont.*

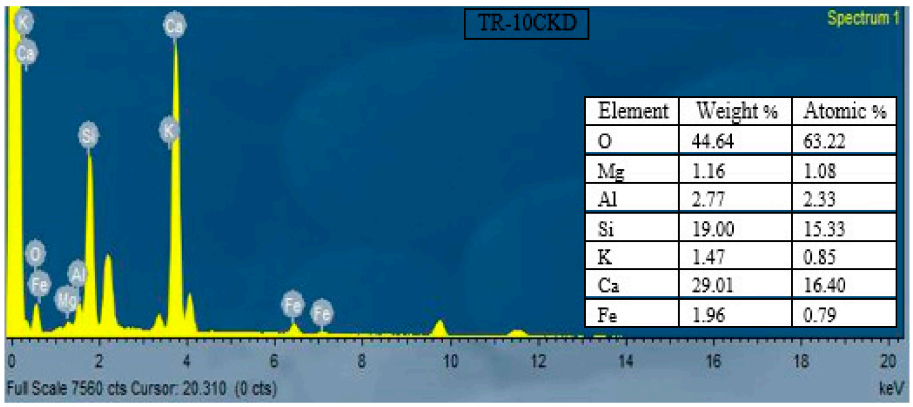

(**d**)

Figure 16. (**a**) EDX patterns of CC mix. (**b**) EDX patterns of NTR50 mix. (**c**) EDX patterns of TRCKD mix. (**d**) EDX patterns of TR-10CKD mix.

Figure 16c indicates that the contained TR CKD shows a more balanced distribution of elements. Compared to NTCR d, a decrease in carbon content is observed, indicating a pathological dispersion of CKD and adequate coverage of rubber crumbs, while the increase in silicon, aluminum, and alkali content is prominent in CKD.

This high silicon content and more uniform distribution of other elements indicates that good integration within the cement matrix for rubber particles has occurred. It seems that treating rubber with CKD enhances the performance of the interfacial transition zone (ITZ) and the overall adhesion of the matrix, which in turn improves the compressive and tensile strength.

Figure 16d illustrates the mix TR-10CKD for treated rubber is shown in addition to replacing 10% of the cement with cement kiln dust. A strong dispersion of CKD particles results in an augmentation of the filler's surface area and consequently reduces stress concentration spots. An increase in CKD leads to a significant improvement, gradually raising the combined water content to 2.5%. This improvement is due to the alkaline content, chlorides, and sulfates present in the cement kiln ash, in addition to the water lime, which acts as a catalyst for GBFS. Increasing the replacement of cement kiln dust by more than 10% leads to a decrease in the combined water content because the amount of ordinary Portland cement is reduced as the amount of cement dust increases. Based on this, the reduction in OPC phases had a significant impact on chemically bound water, due to their hydraulic properties. Among these phases are C3S, β-C2S, C3A, and C4AF.

6. Conclusions

In order to improve environmental sustainability, this study investigates the use of treated crumb rubber as a partial replacement for sand at levels of 25%, 50%, 75%, and 100%, given the importance of engineered cementitious composites (ECC). The compressive strength and overall mechanical performance of ECC were assessed in relation to various curing techniques. Rubber particles (both treated and untreated) were used to partially replace cement and sand in the suggested ECC combinations that included waste materials. These mixtures were evaluated using tests for compressive strength, uniaxial tensile strength, flexural strength, and water absorption. Additionally, to describe the internal morphology and elemental content of specific combinations, microstructural investigations using SEM and EDX were carried out. The main conclusions reached from this research study were as follows:

- The workability of ECC mixtures was affected by the addition of rubber and supplementary materials. Replacing 50% and 100% of sand with untreated rubber reduced

slump by 30% and 50%, respectively. Physically treated rubber increased slump by 42–57%, while chemically treated rubber increased it by 21–50% at 50% replacement. Partial replacement of cement with 10% ESW or CPW raised slump by 43%, and CKD increased it by up to 32% at the same replacement level, with smaller improvements at higher contents.

- When untreated rubber was added to ECC mixtures, their compressive and uniaxial tensile strengths declined. This decline became more noticeable as replacement ratios increased in comparison to the control mixture. In contrast to untreated rubber at the same level, the application of chemically or physically treated rubber at a 50% replacement level enhanced both compressive and uniaxial tensile strengths. The mixture including 50% treated rubber (TR-CKD) with 10% ESW, 10% CKD, and 10% CPW showed a discernible improvement in compressive and uniaxial tensile strengths at 28 days.
- Increasing the replacement ratio of untreated CR in ECC mixtures reduced the compressive strength by up to 33% at a 50% replacement level. In contrast, using 50% physically treated CR with CKD improved the compressive strength by about 20%. Moreover, partial replacement of cement by 10% with ESW, CKD, and CPW enhanced the compressive strength by approximately 15%, 30%, and 18%, respectively.
- ECC mixtures containing untreated rubber exhibited improved bending strength, which increased with higher rubber content. In contrast, using 50% physically or chemically treated rubber reduced flexural strength by 6.3–10.2% and 9.4–28%, respectively. Partial replacement of cement by 10% with ESW, CKD, or CPW in mixtures with 50% treated rubber further decreased bending strength by 11.6%, 8.3%, and 6.7%, respectively.
- Water absorption and sorptivity of ECC mixtures improved with the incorporation of physically treated rubber. Partial replacement of fine aggregate with ESW, CPW, and CKD reduced water absorption by 16.2%, 22%, and 31.4%, respectively. Chemically treated rubber decreased water absorption by 25.7% with NaOH and 12.4% with Na_2SiO_3, while the combination of both treatments slightly increased absorption by 3.3%. Additionally, replacing 10% of cement with ESW, CKD, or CPW reduced water sorptivity by 43%, 22%, and 40%, respectively, whereas exceeding 10% replacement with ESW or CPW increased sorptivity.
- The incorporation of basalt fibers (BF) and steel fibers (S_tF) significantly influenced compressive strength compared to polypropylene fibers (PPF). S_tF-reinforced samples exhibited brittle behavior with surface spalling, whereas BF reduced crack propagation and prevented spalling. Both BF and S_tF enhanced compressive strength by up to 17%.
- Basalt fibers (BF) contributed to the tensile failure pattern in concrete, where fine cracks appeared within the sample. Overall, the addition of BF and S_tF led to significant improvements of 53.33% and 18.33% in flexural strength, respectively.
- BF addition and S_tF in the concrete mixture increased the concrete workability. However, PPF showed lower slump values when compared to BF and S_tF.
- All combinations of released rubber showed a similar pattern of compressive strength losses of 10.25% when exposed to acid; treated rubber mixtures demonstrated the least decline, ranging from 4.4% to 11.6%. The compression strength of TR Na_2SiO_3 was 4.4% higher when subjected to acid assault.
- Low cement replacement levels (10%) with CKD and CPW enhanced compressive strength due to filler effects, matrix densification, and the pozzolanic activity of CPW, with increases of 7.4% and 13% after 120 days, respectively. In contrast, 10% ESW reduced compressive strength by 7.5%. Higher replacement levels (20%) with CKD, CPW, or ESW decreased compressive strength, attributed to increased porosity and poor adhesion caused by micro-cracks and impurities.

- Microscopic examination revealed that untreated rubber increased porosity in ECC, weakening the transition zone and reducing compressive strength. In contrast, cured rubber improved matrix cohesion and transition zone bonding, enhancing overall mechanical properties. Partial replacement of cement with 10% CKD further improved matrix density, bonding, and performance through effective pozzolanic reactions, contributing to the sustainability of ECC.

Overall, rubber treatment significantly contributes to the mechanical properties of engineered cementitious composite (ECC) concrete that includes rubber, specifically through physical treatment. Partial replacement of certain pozzolanic waste materials in specific proportions enhances the performance of ECC. Therefore, adding rubber to mixers in proportions to replace fine aggregates reduces the consumption of natural resources and helps solve the problem of disposing of tires that are harmful to the environment. Additionally, to save energy consumption and reduce the carbon footprint, these materials (ESW, CKD, and CPW) can be used in ECC to lower the overall cost and produce environmentally friendly concrete.

Future Work

As a future extension of this research, it is recommended to quantify surface energy changes through contact angle testing, Zeta potential analysis, or interfacial shear strength testing. In addition, it is recommended to supplement dynamic contact angle data of rubber surfaces and nanoindentation hardness gradients in the interfacial transition zone (ITZ) to confirm the micro-mechanical essence of improved bonding. It is also recommended to extend the sulfate and acid exposure periods to beyond 365 days and supplement with ultrasonic pulse velocity (UPV) and mass change rate data. Life cycle analysis is also recommended for future work to quantify environmental impacts across raw material acquisition, transportation, production, and disposal phases, and to assess potential harmful substance leaching risks.

Author Contributions: Conceptualization, R.A.M.A., M.E.E.-Z. and B.S.A.; methodology, R.A.M.A., M.E.E.-Z. and O.Y.; software, R.A.M.A.; validation, R.A.M.A., O.Y. and B.S.A.; formal analysis, R.A.M.A. and O.Y.; investigation, R.A.M.A. and M.E.E.-Z.; resources, B.S.A. and O.Y.; data curation, B.S.A. and O.Y.; writing—original draft preparation, R.A.M.A., O.Y. and B.S.A.; writing—review and editing, R.A.M.A., M.E.E.-Z., O.Y. and B.S.A.; visualization, M.E.E.-Z.; supervision, M.E.E.-Z. and B.S.A.; project administration, M.E.E.-Z. and B.S.A.; funding acquisition, O.Y. and B.S.A. All authors have read and agreed to the published version of the manuscript.

Funding: This research received no external funding.

Data Availability Statement: All data supporting the findings of this study are available within the manuscript.

Conflicts of Interest: The authors declare that they have no known competing financial interests or personal relationships that could have appeared to influence the work reported in this paper.

References

1. Li, V.C. From micromechanics to structural engineering. *Doboku Gakkai Ronbunshu* **1993**, *1993*, 1–12. [CrossRef]
2. Yoo, D.Y.; Banthia, N. High-performance strain-hardening cementitious composites with tensile strain capacity exceeding 4%: A review. *Cem. Concr. Compos.* **2022**, *125*, 104325. [CrossRef]
3. Su, Y.L.; Wu, C.; Shang, J.Q.; Zhang, P.; Sheikh, S.A. Numerical and theoretical studies for the shear behavior of CFRP plate-ECC-concrete composite interface. *Constr. Build. Mater.* **2023**, *403*, 133156. [CrossRef]
4. Yu, K.; Wang, Y.; Yu, J.; Xu, S. A strain-hardening cementitious composites with the tensile capacity up to 8%. *Constr. Build. Mater.* **2017**, *137*, 410–419. [CrossRef]
5. Zhang, D.; Yu, J.; Wu, H.; Jaworska, B.; Ellis, B.R.; Li, V.C. Discontinuous micro-fibers as intrinsic reinforcement for ductile Engineered Cementitious Composites (ECC). *Compos. B Eng.* **2020**, *184*, 107741. [CrossRef]

6. Ge, W.; Ashour, A.F.; Cao, D.; Lu, W.; Gao, P.; Yu, J.; Ji, X.; Cai, C. Experimental study on flexural behavior of ECC-concrete composite beams reinforced with FRP bars. *Compos. Struct.* **2019**, *208*, 454–465. [CrossRef]
7. Sun, R.; Han, L.; Zhang, H.; Ge, Z.; Guan, Y.; Ling, Y.; Schlangen, E.; Šavija, B. Fatigue life and cracking characterization of engineered cementitious composites (ECC) under flexural cyclic load. *Constr. Build. Mater.* **2022**, *335*, 127465. [CrossRef]
8. Xu, L.; Wang, X.; Dong, B.; Yang, X.; Pan, J. Seismic behaviors of steel-FRP composite bar-reinforced engineered cementitious composites columns under reversed cyclic loads. *Eng. Struct.* **2024**, *316*, 118571. [CrossRef]
9. Zhang, P.; Su, Y.; Liu, Y.; Gao, D.; Sheikh, S.A. Flexural behavior of GFRP reinforced concrete beams with CFRP grid-reinforced ECC stay-in-place formworks. *Compos. Struct.* **2021**, *277*, 114653. [CrossRef]
10. Cai, J.; Pan, J.; Xu, L.; Li, G.; Ma, T. Mechanical behavior of RC and ECC/RC composite frames under reversed cyclic loading. *J. Build. Eng.* **2021**, *35*, 102036. [CrossRef]
11. Jafarian Kafshgarkolaei, H.; Lotfollahi-Yaghin, M.A.; Mojtahedi, A. A modified orthonormal polynomial series expansion tailored to thin beams undergoing slamming loads. *Ocean Eng.* **2019**, *182*, 38–47. [CrossRef]
12. Bagheri, M.; Ranjbar Malidarreh, N.; Ghaseminejad, V.; Asgari, A. Seismic resilience assessment of RC superstructures on long–short combined piled raft foundations: 3D SSI modeling with pounding effects. *Structures* **2025**, *81*, 110176. [CrossRef]
13. Zheng, Y.; Zhang, L.F.; Xia, L.P. Investigation of the behaviour of flexible and ductile ECC link slab reinforced with FRP. *Constr. Build. Mater.* **2018**, *166*, 694–711. [CrossRef]
14. Amiri, M.; Reza Esfahani, M. Effect of using Engineered Cementitious Composites (ECC) on failure behavior of flat slab-column connections. *Structures* **2023**, *47*, 2397–2407. [CrossRef]
15. Hariaravind, G.; Praveenkumar, S.; Sharmila, S.; Shanmugasundaram, N. Behaviour of FRP-ECC-HSC composite stub columns under axial compression: Experimental and mathematical approach. *Constr. Build. Mater.* **2023**, *408*, 133707. [CrossRef]
16. Li, S.; Chan, T.M.; Young, B. Experimental investigation on axial compressive behavior of novel FRP-ECC-HSC composite short column. *Compos. Struct.* **2023**, *303*, 116285. [CrossRef]
17. Lim, C.; Jeong, Y.; Kim, J.; Kwon, M. Experimental study of reinforced concrete beam-column joint retrofitted by CFRP grid with ECC and high strength mortar. *Constr. Build. Mater.* **2022**, *340*, 127694. [CrossRef]
18. Said, S.H.; Abdul Razak, H. Structural behavior of RC engineered cementitious composite (ECC) exterior beam-column joints under reversed cyclic loading. *Constr. Build. Mater.* **2016**, *107*, 226–234. [CrossRef]
19. Dong, B.; Pan, J. Mechanical behaviours of ECC-encased CFST composite column-RECC ring beam connections under axial and eccentric loading. *J. Build. Eng.* **2024**, *82*, 108226. [CrossRef]
20. Meng, Q.; Zaman, I.; Hannam, J.R.; Kapota, S.; Luong, L.; Youssf, O.; Ma, J. Improvement of adhesive toughness measurement. *Polym. Test.* **2011**, *30*, 243–250. [CrossRef]
21. Yi, O.; Mills, J.E.; Zhuge, Y.; Ma, X.; Gravina, R.J.; Youssf, O. Performance of crumb rubber concrete composite-deck slabs in 4-point-bending. *J. Build. Eng.* **2021**, *40*, 102695. [CrossRef]
22. Benazzouk, A.; Douzane, O.; Langlet, T.; Mezreb, K.; Roucoult, J.M.; Quéneudec, M. Physico-mechanical properties and water absorption of cement composite containing shredded rubber wastes. *Cem. Concr. Compos.* **2007**, *29*, 732–740. [CrossRef]
23. Thomas, B.S.; Gupta, R.C. Long term behaviour of cement concrete containing discarded tire rubber. *J. Clean. Prod.* **2015**, *102*, 78–87. [CrossRef]
24. Onuaguluchi, O.; Panesar, D.K. Hardened properties of concrete mixtures containing pre-coated crumb rubber and silica fume. *J. Clean. Prod.* **2014**, *82*, 125–131. [CrossRef]
25. Youssf, O.; Mills, J.E.; Ellis, M.; Benn, T.; Zhuge, Y.; Ma, X.; Gravina, R.J. Practical Application of Crumb Rubber Concrete in Residential Slabs. *Structures* **2022**, *36*, 837–853. [CrossRef]
26. Adesina, A.; Das, S. Performance of engineered cementitious composites incorporating crumb rubber as aggregate. *Constr. Build. Mater.* **2021**, *274*, 122033. [CrossRef]
27. Huang, X.; Ranade, R.; Ni, W.; Li, V.C. On the use of recycled tire rubber to develop low E-modulus ECC for durable concrete repairs. *Constr. Build. Mater.* **2013**, *46*, 134–141. [CrossRef]
28. Sait Cülfik, M. Effect of elevated temperatures on the residual mechanical properties of high-performance mortar. *Cem. Concr. Res.* **2002**, *32*, 809–816. [CrossRef]
29. Li, G.; Stubblefield, M.A.; Garrick, G.; Eggers, J.; Abadie, C.; Huang, B. Development of waste tire modified concrete. *Cem. Concr. Res.* **2004**, *34*, 2283–2289. [CrossRef]
30. Najim, K.B.; Hall, M.R. Crumb rubber aggregate coatings/pre-treatments and their effects on interfacial bonding, air entrapment and fracture toughness in self-compacting rubberised concrete (SCRC). *Mater. Struct./Mater. Constr.* **2013**, *46*, 2029–2043. [CrossRef]
31. Ottman, N.; Ruokolainen, L.; Suomalainen, A.; Sinkko, H.; Karisola, P.; Lehtimäki, J.; Lehto, M.; Hanski, I.; Alenius, H.; Fyhrquist, N. Soil exposure modifies the gut microbiota and supports immune tolerance in a mouse model. *J. Allergy Clin. Immunol.* **2019**, *143*, 1198–1206.e12. [CrossRef]
32. Raffoul, S.; Garcia, R.; Pilakoutas, K.; Guadagnini, M.; Medina, N.F. Optimisation of rubberised concrete with high rubber content: An experimental investigation. *Constr. Build. Mater.* **2016**, *124*, 391–404. [CrossRef]

33. Abd-Elaal, E.S.; Araby, S.; Mills, J.E.; Youssf, O.; Roychand, R.; Ma, X.; Zhuge, Y.; Gravina, R.J. Novel approach to improve crumb rubber concrete strength using thermal treatment. *Constr. Build. Mater.* **2019**, *229*, 116901. [CrossRef]
34. Kashani, A.; Ngo, T.D.; Hemachandra, P.; Hajimohammadi, A. Effects of surface treatments of recycled tyre crumb on cement-rubber bonding in concrete composite foam. *Constr. Build. Mater.* **2018**, *171*, 467–473. [CrossRef]
35. Alwi Assaggaf, R.; Uthman Al-Dulaijan, S.; Maslehuddin, M.; Baghabra Al-Amoudi, O.S.; Ahmad, S.; Ibrahim, M. Effect of different treatments of crumb rubber on the durability characteristics of rubberized concrete. *Constr. Build. Mater.* **2022**, *318*, 126030. [CrossRef]
36. Ul Aleem, M.A.; Siddique, M.S.; Farooq, S.H.; Usman, M.; Ahsan, M.H.; Hussain, M.; Hanif, A. Axial compressive behavior of concrete incorporating crumb rubber pretreated with waste quarry dust. *J. Build. Eng.* **2022**, *59*, 105086. [CrossRef]
37. Collins, R.J.; Emery, J.J. *Kiln Dust-Fly Ash Systems for Highway Bases and Subbases: Final Report*; Federal Highway Administration: Washington, DC, USA, 1983.
38. Al-Harthy, A.S.; Taha, R.; Al-Maamary, F. Effect of cement kiln dust (CKD) on mortar and concrete mixtures. *Constr. Build. Mater.* **2003**, *17*, 353–360. [CrossRef]
39. Pizon, J.; Lazniewska-Piekarczyk, B. Efficiency assessment of accelerating admixtures and cement kiln dust with cooperation with different phase composition slag blended cements. *IOP Conf. Ser. Mater. Sci. Eng.* **2019**, *603*, 032088. [CrossRef]
40. Ravindrarajah, R.S. Usage of cement kiln dust in concrete. *Int. J. Cem. Compos. Lightweight Concr.* **1982**, *4*, 95–102. [CrossRef]
41. Detwiler, R.J.; Bhatty, J.I.; Battacharja, S. *Supplement Cementing Materials for Use in Blended Cement*; PCA: Skokie, IL, USA, 1996.
42. Siddique, R. *Waste Material and By-Products in Concrete*; Springer: Berlin/Heidelberg, Germany, 2008.
43. Batis, G.; Rakanta, E.; Sideri, E.; Chaniotakis, E.; Papageorgiou, A. Advantages of simultaneous use of cement kiln dust and blast furnace slag. In *Challenges of Concrete Construction: Volume 5, Sustainable Concrete Construction: Proceedings of the International Conference Held at the University of Dundee, Scotland, UK, 9–11 September 2002*; Thomas Telford Publishing: London, UK, 2002; pp. 205–212.
44. Daugherty, K.E.; Funnell, J.E. The incorporation of low levels of by-products in portland cement and the effects on cement quality. *Cem. Concr. Aggreg.* **1983**, *5*, 14–20. [CrossRef]
45. Justnes, H. *Hardening Accelerators for Fly Ash Blended Cement*; FA 1 Environmentally friendly concrete. SP 1.1 Low carbon-footprint binder systems; SINTEF: Trondheim, Norway, 2015.
46. Ji, Y.; Chen, A.; Chen, Y.; Han, X.; Li, B.; Gao, Y.; Liu, C.; Xie, J. A state-of-the-art review of concrete strength detection/monitoring methods: With special emphasis on PZT transducers. *Constr. Build. Mater.* **2023**, *362*, 129742. [CrossRef]
47. Vasudevan, G.; Chan Wei, S. Utilisation of Eggshell Powder (ESP) as Partial Replacement of Cement Incorporating Superplasticizer. *IOP Conf. Ser. Mater. Sci. Eng.* **2020**, *840*, 012016. [CrossRef]
48. Jamshaid, H.; Mishra, R. A green material from rock: Basalt fiber—A review. *J. Text. Inst.* **2016**, *107*, 923–937. [CrossRef]
49. Yang, E.-H. Designing Added Functions in Engineered Cementitious Composites. University of Michigan, Ann Arbor, MI, USA, 2008.
50. Yang, E.-H.; Li, V.C. Strain-hardening fiber cement optimization and component tailoring by means of a micromechanical model. *Constr. Build. Mater.* **2010**, *24*, 130–139. [CrossRef]
51. Felekoglu, B.; Tosun-Felekoglu, K.; Ranade, R.; Zhang, Q.; Li, V.C. Influence of matrix flowability, fiber mixing procedure, and curing conditions on the mechanical performance of HTPP-ECC. *Compos. B Eng.* **2014**, *60*, 359–370. [CrossRef]
52. Kakooei, S.; Akil, H.M.; Jamshidi, M.; Rouhi, J. The effects of polypropylene fibers on the properties of reinforced concrete structures. *Constr. Build. Mater.* **2012**, *27*, 73–77. [CrossRef]
53. Zhang, P.; Li, Q.F. Effect of polypropylene fiber on durability of concrete composite containing fly ash and silica fume. *Compos. B Eng.* **2013**, *45*, 1587–1594. [CrossRef]
54. Ramezanianpour, A.A.; Esmaeili, M.; Ghahari, S.A.; Najafi, M.H. Laboratory study on the effect of polypropylene fiber on durability, and physical and mechanical characteristic of concrete for application in sleepers. *Constr. Build. Mater.* **2013**, *44*, 411–418. [CrossRef]
55. Youssf, O.; Hassanli, R.; Mills, J.E. Retrofitting square columns using FRP-confined crumb rubber concrete to improve confinement efficiency. *Constr. Build. Mater.* **2017**, *153*, 146–156. [CrossRef]
56. Helal, K.A.; Tahwia, A.M.; Youssf, O. Performance of eco-friendly ECC made of pre-treated crumb rubber and waste quarry dust. *J. Build. Eng.* **2024**, *97*, 110820. [CrossRef]
57. Japan Society of Civil Engineering. *Standard Specifcations and Guidelines*; Japan Society of Civil Engineering: Tokyo, Japan, 2008.
58. Aiken, T.A.; Kwasny, J.; Sha, W.; Tong, K.T. Mechanical and durability properties of alkali-activated fly ash concrete with increasing slag content. *Constr. Build. Mater.* **2021**, *301*, 124330. [CrossRef]
59. *ASTM C1585-13*; Standard Test Method for Measurement of Rate of Absorption of Water by Hydraulic-Cement Concretes. ASTM Int.: West Conshohocken, PA, USA, 2013. [CrossRef]
60. Alsaadawi, M.M.; Amin, M.; Tahwia, A.M. Thermal, mechanical and microstructural properties of sustainable concrete incorporating Phase change materials. *Constr. Build. Mater.* **2022**, *356*, 129300. [CrossRef]

61. Awan, H.H.; Javed, M.F.; Yousaf, A.; Aslam, F.; Alabduljabbar, H.; Mosavi, A. Experimental evaluation of untreated and pretreated crumb rubber used in concrete. *Crystals* **2021**, *11*, 558. [CrossRef]
62. Guo, S.; Dai, Q.; Si, R.; Sun, X.; Lu, C. Evaluation of properties and performance of rubber-modified concrete for recycling of waste scrap tire. *J. Clean. Prod.* **2017**, *148*, 681–689. [CrossRef]
63. Khalil, K.A.; Abd-El-Hameed, N.M. Physicochemical Characteristics of Slag Rich Cement Pastes Incorporated by-pass Cement Dust. *Egypt. J. Chem.* **2016**, *59*, 491–507. [CrossRef]
64. Wang, K.; Konsta-Gdoutos, M.S.; Shah, S.P. Hydration, rheology, and strength of ordinary portland cement (OPC)-cement kiln dust (CKD)-slag binders. *ACI Mater. J.* **2002**, *99*, 173–179.
65. Ramesh, B.; Eswari, S. Mechanical behaviour of basalt fibre reinforced concrete: An experimental study. *Mater. Today Proc.* **2020**, *43*, 2317–2322. [CrossRef]
66. Uygunoğlu, T. Investigation of microstructure and flexural behavior of steel-fiber reinforced concrete. *Mater. Struct.* **2008**, *41*, 1441–1449. [CrossRef]
67. Afroughsabet, V.; Ozbakkaloglu, T. Mechanical and Durability Properties of High-Strength Concrete Containing Steel and Polypropylene Fibers. *Constr. Build. Mater.* **2015**, *94*, 73–82. [CrossRef]
68. Kizilkanat, A.B.; Kabay, N.; Akyüncü, V.; Chowdhury, S.; Akça, A.H. Mechanical properties and fracture behavior of basalt and glass fiber reinforced concrete: An experimental study. *Constr. Build. Mater.* **2015**, *100*, 218–224. [CrossRef]
69. Vafaei, D.; Hassanli, R.; Ma, X.; Duan, J.; Zhuge, Y. Sorptivity and mechanical properties of fiber-reinforced concrete made with seawater and dredged sea-sand. *Constr. Build. Mater.* **2021**, *270*, 121436. [CrossRef]
70. Yu, Z.; Liu, X.; Xue, Q.; Shen, X. New perspective to improve the sulfate attack resistance of mortar by coral sand. *J. Build. Eng.* **2023**, *71*, 106483. [CrossRef]
71. Li, Y.; Zhang, X.; Wang, R.; Lei, Y. Performance enhancement of rubberised concrete via surface modification of rubber: A review. *Constr. Build. Mater.* **2019**, *227*, 116691. [CrossRef]
72. Bisht, K.; Ramana, P.V. Evaluation of mechanical and durability properties of crumb rubber concrete. *Constr. Build. Mater.* **2017**, *155*, 811–817. [CrossRef]
73. Santarelli, M.L.; Sbardella, F.; Zuena, M.; Tirillò, J.; Sarasini, F. Basalt fiber reinforced natural hydraulic lime mortars: A potential bio-based material for restoration. *Mater. Des.* **2014**, *63*, 398–406. [CrossRef]
74. Richerson, D.W.; Lee, W.E. *Modern Ceramic Engineering: Properties, Processing, and Use in Design*; CRC Press: Boca Raton, FL, USA, 2018.
75. Shen, L.; Yao, X.; Di Luzio, G.; Jiang, M.; Han, Y. Mix optimization of hybrid steel and polypropylene fiber-reinforced concrete for anti-thermal spalling. *J. Build. Eng.* **2023**, *63*, 105409. [CrossRef]
76. Xu, L.; Deng, F.; Chi, Y. Nano-mechanical behavior of the interfacial transition zone between steel-polypropylene fiber and cement paste. *Constr. Build. Mater.* **2017**, *145*, 619–638. [CrossRef]
77. Barrentine, L.B. *An Introduction to Design of Experiments: A Simplified Approach*; ASQ Quality Press: Milwaukee, WI, USA, 1999.

Disclaimer/Publisher's Note: The statements, opinions and data contained in all publications are solely those of the individual author(s) and contributor(s) and not of MDPI and/or the editor(s). MDPI and/or the editor(s) disclaim responsibility for any injury to people or property resulting from any ideas, methods, instructions or products referred to in the content.